IVYSPRING INTERNATIONAL PUBLISHER

Theranostics

2018; 8(4): 921-940. doi: 10.7150/thno.22182

Research Paper

Cancer-associated Fibroblast-derived IL-6 Promotes Head and Neck Cancer Progression via the Osteopontin-NF-kappa B Signaling Pathway

Xing Qin[1], Ming Yan[1], Xu Wang[1], Qin Xu[1, 2], Xiaoning Wang[1], Xueqin Zhu[1], Jianbo Shi[1], Zhihui Li[1], Jianjun Zhang[1]✉, Wantao Chen[1, 2]✉

1. Department of Oral and Maxillofacial-Head & Neck Oncology, Ninth People's Hospital, Shanghai Jiao Tong University School of Medicine, Shanghai, 200011, PR China;
2. Shanghai Key Laboratory of Stomatology & Shanghai Research Institute of Stomatology; National Clinical Research Center of Stomatology, Shanghai, 200011, PR China.

✉ Corresponding authors: **Wantao Chen**, Ninth People's Hospital, Shanghai Jiao Tong University School of Medicine, 639 Zhizaoju Road, Shanghai 200011, China; Telephone: (86) 21-23271699-5210; Fax: (86) 21-63135412; E-mail: chenwantao196323@sjtu.edu.cn. **Jianjun Zhang**, Ninth People's Hospital, Shanghai Jiao Tong University School of Medicine, 639 Zhizaoju Road, Shanghai 200011, China; Telephone: (86) 21-23271699-6509; E-mail: zjjshuobo@163.com.

Received: 2017.08.01; Accepted: 2017.11.02; Published: 2018.01.01

Abstract

Osteopontin (OPN), a chemokine-like protein, plays a crucial role in the proliferation and metastasis of various cancers. However, how tumor stroma modulates the expression of neoplastic OPN and the multifaceted roles of OPN in head and neck cancer (HNC) are unclear. In this study, we tried to investigate the bridging role of OPN between tumor stroma and cancer cells.

Methods: Immunohistochemical staining and quantitative real-time PCR were used to detect OPN expression in HNC tissues, and the correlations between OPN expression and clinicopathologic features were then analyzed. We used a co-culture assay to study the modulatory role of IL-6 on OPN expression and immunoprecipitation analysis was used to determine the endogenous interaction between OPN and integrin αvβ3. Furthermore, a xenograft assay was carried out to confirm the tumor-promoting role and the potential therapeutic value of OPN in HNC.

Results: We found that OPN was significantly up-regulated in HNCs, and the elevated OPN was correlated with poor prognosis. Moreover, we identified IL-6 secreted by cancer-associated fibroblasts (CAFs) as the major upstream molecule that triggers the induction of neoplastic OPN. As such, during the interaction of fibroblasts and cancer cells, the increased neoplastic OPN induced by stromal IL-6 accelerated the growth, migration and invasion of cancer cells. More importantly, we also showed that soluble OPN could promote HNC progression via the integrin αvβ3-NF-kappa B pathway, and the combination of OPN and IL-6 had a better prognostic and diagnostic performance in HNC than either molecule alone.

Conclusion: Our study identified a novel modulatory role for OPN in HNC progression and further demonstrated that the combination of OPN and IL-6 might be a promising prognostic and diagnostic indicator as well as a potential cancer therapeutic target.

Key words: IL-6; Osteopontin; NF-kappa B; Head and Neck Cancer; Cancer-associated fibroblasts.

Introduction

Head and neck cancer (HNC), which is predominantly comprised of squamous cell carcinoma, is a common and aggressive malignancy with high morbidity and mortality rates [1, 2]. Current treatments for HNC patients are primarily based on tumor stage and anatomic location, and therapies based on the underlying biology are rare [3]. Despite advancements in techniques and supportive care, which have improved the quality of life for patients with HNC, the overall prognosis is still poor due to local recurrence and distant metastasis after surgery [3]. Thus, a better understanding of the molecular

mechanisms underlying HNC progression is urgently needed to improve prevention, diagnosis, and personalized treatment for patients.

Osteopontin (OPN, also known as ETA1 and encoded by SPP1), which was identified as a phosphoprotein secreted by malignant epithelial cells, T lymphocytes, and osteoblasts, is a multifunctional extracellular matrix (ECM) protein [4, 5]. OPN has been reported to play multifaceted roles in regulating bone resorption, matrix turnover, and inflammatory and immune responses [6, 7]. Clinical reports have found that a range of malignant tumor tissues showed higher OPN expression than adjacent normal tissue, and the high expression of OPN was correlated with advanced stage, metastasis and poor prognosis [8, 9]. Similarly, OPN activates multiple signaling pathways that regulate the expression of various oncogenic and angiogenic molecules to promote tumor growth, metastasis and angiogenesis [9-11]. OPN has been identified as a plasma biomarker for predicting the prognosis and metastasis of many cancer types, including HNC [12, 13]. Although the tumor-promoting molecular mechanisms of OPN have been investigated in other cancers, they are still unclear in HNC.

Accumulating evidences have indicated that tumor growth and metastasis are highly dependent on complex dynamic interactions between tumor cells and tumor stroma, mediated by direct cell-cell contact and secreted growth factors and cytokines [14, 15]. OPN is abundant in the stroma that is present within the tumor microenvironment. Recent findings suggested that tumor-derived OPN instigates mesenchymal stem cell trafficking to the tumor microenvironment [16, 17], and neoplastic OPN can modulate the phenotype of cancer-associated fibroblasts (CAFs) and enhance angiogenesis by up-regulating COX-2 expression in macrophages [18, 19]. Conversely, it was reported that OPN derived from senescent fibroblasts stimulates preneoplastic cell growth through the CD44 receptor and MAPK activation pathway [20, 21], macrophage-secreted OPN binds to CD44s on the tumor cells and promotes tumor invasion and clonal growth [10], and OPN excretion from hepatic stellate cells promotes the migration of hepatocellular carcinoma cells [22]. Collectively, these studies highlight the importance of stromal OPN in tumorigenesis and tumor progression. CAFs, major components of tumor stroma, are key players in regulating tumor progression [14, 15]. However, the role of CAFs in OPN-mediated tumor development is still unclear, especially in HNC.

The nuclear factor kappa B (NF-kappa B) pathway is a major proinflammatory signaling pathway, and evidence has suggested that this signaling pathway plays a critical role in carcinogenesis, protection from apoptosis and chemoresistance in multiple types of cancer [23]. NF-kappa B, which is present in the cytoplasm, can enter the nucleus to regulate the expression of genes involved in cell growth, invasion and metastasis after the degradation of phosphorylated IκBα [24]. OPN has been recognized as an important proinflammatory cytokine with pleiotropic functions [7]. Secreted OPN activates the NF-kappa B signaling pathway primarily by binding to integrin αvβ3 and eventually results in tumor progression [25-27]. Interestingly, OPN was shown to increase tumor growth via activation of the CD44/NF-kappa B pathway in cells with low integrin β3 levels in breast cancer [28]. However, it is still unclear whether the NF-kappa B signaling pathway is involved in secreted OPN-mediated HNC progression.

In this study, we showed that OPN expression was increased in tumor tissues and plasma of HNC patients and was associated with tumor stage and metastasis. We then fully analyzed the mechanisms underlying alteration in OPN levels and the functional role of secreted OPN in HNC cell proliferation, migration and invasion *in vitro* and *in vivo*. Additionally, our data revealed that CAF-secreted IL-6 promoted cancer cell growth and metastasis through the induction of neoplastic OPN transcription. Our findings suggested that IL-6-mediated expression of neoplastic OPN could accelerate HNC progression via the NF-kappa B signaling pathway and that OPN in combination with IL-6 might serve as a promising prognostic indicator and potential therapeutic target for HNC.

Materials and Methods

Ethics

The Ethics Committee of Shanghai Jiao Tong University approved our study. All participants provided written informed consent prior to enrollment. All experimental methods complied with the Helsinki Declaration. All animal studies have been approved by the Shanghai Jiao Tong University Institute Animal Care and Use Committee, and all mice were kept in the Shanghai Jiao Tong University School of Medicine animal facilities.

Patients and specimens

All the samples were collected from the Department of Oral and Maxillofacial-Head and Neck Oncology, Ninth People's Hospital, Shanghai Jiao Tong University School of Medicine (Shanghai, China). The clinical samples used in this study are as follows: 60 pairs of HNC tissues and adjacent normal

tissues; total RNAs from 110 HNC tissues and 96 normal oral epithelial tissues; 137 plasma samples from HNC patients and 140 plasma samples from healthy individuals. Detailed information on these samples is available in the Supplementary Materials and methods.

Cell cultures

As previously described [29], the human HNC cell lines HN4, HN6 and HN30 were kindly provided by the University of Maryland Dental School, USA. SCC-4, SCC-9, SCC-25 and CAL-27 cells were purchased from the American Type Culture Collection (ATCC, USA). The human HB cell line was derived from HIOEC by treatment with benzo[a]pyrene [30] and the Rca-T cell line was purified from tongue squamous cell carcinoma tissues induced by adding 4-nitroquinoline-1-oxide into Sprague-Dawley rats' drinking water [31]. CAFs and normal fibroblasts (NFs) were isolated from tumor and adjacent normal tissues of HNC patients by primary culture and were identified by the presence of CAF-specific markers (α-SMA, Vimentin). All these cells except SCC-4, SCC-9 and SCC-25 were cultured in Dulbecco's modified Eagle's medium (DMEM; GIBCO-BRL, USA) supplemented with 10% heat-inactivated FBS (GIBCO-BRL), penicillin (100 units/mL), and streptomycin (100 μg/mL) at 37°C in a humidified 5% CO_2 atmosphere, while SCC-4, SCC-9 and SCC-25 cells were maintained in DMEM/F12 medium containing 10% FBS. In addition, normal primary head and neck epithelial cells were cultured in keratinocyte serum-free medium (KSF; GIBCO-BRL, USA) with 0.2 ng/mL recombinant epidermal growth factor (rEGF; Invitrogen, USA).

Immunohistochemical analysis

Briefly, paraffin-embedded 3 μm thick sections were deparaffinized, rehydrated, submerged into citric acid buffer for heat-induced antigen retrieval, immersed in 0.3% hydrogen peroxide to block endogenous peroxidase activity, blocked with 3% bovine serum albumin, incubated with primary antibodies at 4°C overnight and developed using the DAKO ChemMate Envision Kit/HRP (Dako-Cytomation, USA). The sections were then counterstained with hematoxylin, dehydrated, cleared and mounted. The tissues exhibiting brown staining in the cytoplasm, nucleus or membrane were considered positive. Five targeted areas of each section were randomly selected under the same conditions for further analysis. The integrated optical density (IOD) of protein expression was quantitatively determined using Image-Pro Plus 6.0 software and calculated with the following formula: MOD = IOD SUM / area SUM (MOD: mean optical density; IOD SUM: the accumulative IOD of targeted areas in one photo; area SUM: the sum of targeted areas). See Supplementary Materials and methods for the antibodies used.

RNA extraction and real-time PCR analysis

Total RNA was extracted with TRIzol Reagent (Invitrogen, USA) and cDNA was synthesized using the PrimerScript RT reagent Kit (Takara, Japan). All real-time PCR reactions were performed using an ABI StepOne real-time PCR system (Life Technologies, USA) and the SYBR Premix Ex Taq reagent kit (Takara, Japan). The reaction was performed as described previously [29] and amplified PCR products were quantified and normalized using β-actin as a control. The PCR primers are described in Table S1.

Western blot analysis

Cells were harvested at the indicated times and rinsed twice with PBS. Cell extracts were prepared with SDS lysis buffer (Beyotime, China) and centrifuged at 14,000 × g for 10 min at 4°C. In addition, the NE-PER™ Nuclear and Cytoplasmic Extraction Reagents (Thermo Fisher, USA) were used for separation and preparation of cytoplasmic and nuclear extracts from cultured cells. Protein samples (40 μg) were electrophoresed using 10% or 15% polyacrylamide gels and transferred to 0.45 μm PVDF membranes (Merck Millipore, USA). After the membranes were blocked with 5% BSA for 1 h at room temperature, the blots were probed with primary antibody. GAPDH and H3 histone were used throughout as loading controls. Secondary antibodies (Sigma, USA; 1:10,000) were labeled with IR Dyes. Signals were observed using an Odyssey Infrared Imaging System (Biosciences, USA). See Supplementary Materials and methods for antibodies used.

ELISA analysis

Culture media of 1×10^6 cells were collected separately after incubation for 72 h and then centrifuged at 10,000 × g for 10 min at 4°C. The supernatant OPN and IL-6 concentrations and the plasma OPN and IL-6 levels in patients with HNC were assessed using the Human OPN ELISA kit (Boster, China) and human IL-6 ELISA kit (Boster, China). Moreover, the mouse OPN ELISA kit (Boster, China) was used to measure the plasma OPN level of nude mice. The OPN and IL-6 concentration in culture media or plasma were calculated according to the formula of the standard curve. See Supplementary Materials and methods for detailed methods.

Immunofluorescence

After the pretreatment as indicated, the cells grown on cover slips were fixed with 4% paraformaldehyde and permeabilized with 0.1% Triton X-100. After the cells were blocked in 3% BSA for 30 min, they were incubated with α-SMA antibody (Abcam, USA; 1:100), Vimentin antibody (Sigma, USA; 1:100) and p65 antibody (CST, USA; 1:800) overnight at 4°C, then washed and incubated for 30 min with an Alexa Fluor 488-conjugated anti-mouse IgG $F(ab')_2$ fragment (Invitrogen, USA; 1:200) or an Alexa Fluor 549-conjugated anti-mouse IgG $F(ab')_2$ fragment (Invitrogen, USA; 1:200) at room temperature in the dark. Cells were co-stained with 4′, 6-diamidino-2-phenylindole (DAPI; Invitrogen, USA; 1:300) to detect nuclei. Cells were observed and imaged using a TCS SP2 laser-scanning confocal microscope (Leica Microsystems, Germany).

Co-culture assay

The co-culture assay was established using transwell membranes (pores 0.4 μm, Merck Millipore, USA). Fibroblasts (2×10^4 cells in 600 μL DMEM medium containing 5% FBS) were plated on the bottom of a 24-well tissue culture plate, and 1×10^4 tumor cells in 300 μL DMEM medium containing 5% FBS were seeded on the transwell membranes. Experiments were performed after the cells were incubated for 72 h, and the different cell types were collected separately for further experiments.

Cell proliferation analysis

Tumor cells were transfected with OPN-expressing plasmid or OPN-specific siRNA in advance. Twenty-four hours later, tumor cells were seeded onto 96-well plates at a density of 1,000 cells in each well in triplicate. The cell proliferation assay was performed with the Cell Counting Kit-8 (Dojindo, Kumamoto, Japan) as described previously [32].

For analysis of tumor cell proliferation in a co-culture system, tumor cells were stably transfected with luciferase cDNA in advance. During the co-culture period, the tumor cell growth was monitored daily by measuring luciferase activity using a Luciferase Assay System (Promega Corporation, USA).

Wound-healing assay

Tumor cells were plated in 6-well plates, transfected or pre-treated as indicated, and cultured to confluency. Cells were serum-starved and scraped with a P200 tip (time 0), washed with PBS, and incubated with serum-free DMEM. Pictures of 5 non-overlapping fields were taken at 24 h.

Transwell migration and invasion assay

The cell migration assay was performed with transwell chamber (pores 0.8 μm, Merck Millipore, USA), while the cell invasion assay was implemented with Matrigel (BD Biosciences, USA) coated on the upper surface of the transwell chamber (pores 0.8 μm, Merck Millipore, USA). Cells that migrated or invaded through the membrane were fixed and stained with crystal violet. Images of five randomly selected fields of the fixed cells were captured, and the cells were counted. See Supplementary Materials and methods for detailed methods.

For the cell migration and invasion assay in the co-culture system, the mixed cells (the tumor cells were stably transfected with luciferase cDNA in advance) were resuspended in serum-free DMEM and then cultured in the upper chamber for 24 h. The cells that migrated or invaded through the membrane were isolated by the trypsin digestion method and quantified by measuring luciferase activity using a Luciferase Assay System (Promega Corporation, USA).

Co-Immunoprecipitation (Co-IP) analysis

Cells were lysed using IP buffer (1% Triton X-100, 150 mM NaCl, 10 mM Tris, pH 7.4, 1 mM EDTA, 1 mM EGTA, pH 8.0, 0.2 mM sodium orthovanadate, 1 mM phenylmethanesulfonyl fluoride (PMSF), 0.5% protease inhibitor cocktail, and 0.5% IGEPAL CA-630). Cell lysates were centrifuged at 12,000 × g for 30 min at 4°C, and the supernatants were incubated with specific antibodies as indicated overnight at 4°C followed by incubation with protein A/protein G-coated agarose beads (Merck) for an additional 4 h at 4°C. After the samples were washed thrice with ice-cold IP buffer and the supernatants were removed by centrifugation at 1,000 × g for 2 min, the proteins were precipitated individually or co-precipitated. The proteins were then separated from the beads using immunoblotting loading buffer for 5 min at 95°C. The supernatants were collected for subsequent immunoblotting analysis with the indicated antibodies.

NF-kappa B-response luciferase reporter assay

Tumor cells or 293T cells (2×10^5) were plated in a 6-well dish and transfected with the NF-kappa B-response luciferase plasmid using Lipofectamine 2000 reagent (Invitrogen, USA) according to the manufacturer's instructions. The cells were co-transfected with the pPenilla Renilla luciferase reporter to normalize for transfection efficiency. Six hours after transfection, the transfection medium was replaced with fresh medium, and the cells were culture for another 24 h. The cells were pre-treated

with external stimulus for 12 h and harvested in passive lysis buffer. Finally, the luciferase activity was measured using the Dual Luciferase System (Promega, USA).

Tumorigenicity assay *in vivo*

To evaluate the tumor promoting role of OPN *in vivo*, a HNC xenograft model was implemented in BALB/C nude mice (4-weeks-old). Briefly, a total of 1×10^6 CAL-27 cells or OPN-expressing CAL-27 cells in 100 μL serum-free DMEM were subcutaneously injected into the left and right buttocks. For the anti-tumor effects of neutralized antibodies, 5×10^5 CAL-27 cells mixed with 3×10^5 NFs in 100 μL serum-free DMEM were subcutaneously injected into the left and right buttocks. Three days after the injections, all mice were divided randomly into 4 groups (4 mice per group) and were treated with neutralized antibodies (anti-OPN, anti-IL-6 or anti-OPN plus anti-IL-6) every 3 days. As previously noted [33], the tumor volume was measured every 3 day by the following formula: tumor volume = length × width × width / 2. After treatment for 15 days, the animals were sacrificed and the tumor volume and tumor weight were measured. The tumor growth curve was plotted using the seeding day as the horizontal axis and the tumor volume as the vertical axis.

Experimental metastasis assay

As previously described [34], Rca-T cell line was used to establish the HNC experimental metastasis model. A total number of 1×10^6 Rca-T cells or OPN-expressing Rca-T cells in 200 μL serum-free DMEM were injected intravenously into the lateral tail vein of the 4-week-old athymic mice. Two weeks later, the animals were sacrificed and the murine lungs were fixed in neutral-buffered formalin, embedded in paraffin, and cut into 3 μm sections for further experiments.

Statistical analyses

Statistical analyses were performed using the Statistical Package for Social Sciences Version 19.0 (SPSS19.0). Student's t-test and one-way ANOVA were used to compare the means of 2 groups or more. Mann-Whitney U-test and Kruskal-Wallis test were used to analyze the data of the associations between OPN mRNA or plasma OPN levels and clinical parameters. The correlation was determined by Pearson analysis. The log-rank test was used to assess the survival differences and Kaplan-Meier survival analyses were used to estimate the prognostic and diagnostic value. The Cox proportional hazards model was used for multivariate analyses, and all potential prognostic factors with p values<0.05 from the univariate analysis were incorporated into multivariate analyses. p<0.05 were considered statistically significant.

The detailed methods for plasmid construction, lentivirus package, siRNA and plasmid transfection, colony formation assay, ChIP assay etc. are described in Supplementary Material and methods.

Results

Overexpression of OPN in HNC indicates malignant transformation

In our previous study [34], we found that OPN was up-regulated in HNC and was characterized as a secreted ECM component. Then, we accessed information regarding OPN expression level provided by the Cancer Genome Atlas (TCGA), and the results indicated that the OPN gene was expressed at high levels in HNC tissues compared with normal tissues (Figure S1). To verify the accuracy of these results, we performed immunohistochemical staining to detect the OPN expression in HNC. Notably, OPN was highly up-regulated in HNC tissues compared with adjacent normal tissues and normal epithelial tissues (Figure 1A). Thereafter, the OPN expression level was tested in 60 paired HNC samples using real-time PCR and in 12 paired HNC samples by western blotting. The data revealed that OPN expression level was increased in HNC tissues compared with adjacent normal tissues (Figure 1B, C).

To further investigate the correlations between OPN expression and the malignant transformation of HNC, we quantified the OPN mRNA levels in expanded HNC cohorts using real-time PCR. Consistent with the above data, OPN was shown to be up-regulated in 110 HNC samples compared with 96 normal oral epithelial tissues (Figure 1D). As shown in Table 1, the OPN expression was significantly correlated with smoking, larger tumor size (greater than 4 cm in diameter), lymph node metastasis and advanced tumor stage. Moreover, Kaplan-Meier analyses and COX regression analyses revealed that OPN expression was significantly correlated with poor overall survival in HNC patients and was an independent predictor of overall survival in HNC (Figure 1E and Table 2). In addition, the secreted OPN levels were also measured in the plasma of HNC patients and heathy controls. We found that the plasma OPN was elevated in HNC patients (Figure 1F) and was significantly decreased 3 or 4 weeks after surgery compared with pre-surgery status (Figure 1G). Similarly, positive associations were also identified between plasma OPN level and smoking, larger tumor size (greater than 4 cm in diameter), lymph node metastasis and advanced tumor stage

(Figure 1H, S2). These data support an association between up-regulated OPN and advanced HNC malignant transformation and suggest the potential value of OPN as a prognostic biomarker and therapeutic target.

Table 1. Relationship between *OPN* mRNA level and clinicopathologic features (N=110)

Characteristics	No. of Patients		*OPN* △Ct[a] Mean ± SD	*Non-parametric test value*	*P value*
	No.	%			
Age (years)					
≥ 60	45	49.9	1.28 ± 2.06	*Z = -0.781*	*0.435*
< 60	65	59.1	1.65 ± 2.37		
Gender					
Male	66	60.0	1.47 ± 2.16	*Z = -0.061*	*0.951*
Female	44	40.0	1.55±2.41		
Smoking history					
Nonsmoker	57	51.8	2.30 ± 2.38	*Z = -3.604*	*0.001*
Smoker	53	48.2	0.64 ± 1.75		
Alcohol history					
Nondrinker	77	70.0	1.74 ± 2.12	*Z = -1.608*	*0.108*
Drinker	33	30.0	0.94 ± 2.47		
Tumor size (cm)					
≤ 4	54	49.1	2.48 ± 2.33	*Z = -4.431*	*0.000*
> 4	56	50.9	0.55 ± 1.71		
Lymph node metastasis					
pN1 to pN2	52	47.3	0.32 ± 1.71	*Z = -5.125*	*0.000*
pN0	58	52.7	2.56 ± 2.16		
TNM stage					
Ⅰ	21	19.1	4.71 ± 1.62	*H = 48.391*	*0.000*
Ⅱ	19	17.3	1.12 ± 1.24		
Ⅲ	31	28.2	1.04 ± 1.66		
Ⅳ	39	35.4	0.32 ± 1.70		
Pathological differentiation					
Well	67	60.9	1.74 ± 2.22	*Z = -1.822*	*0.068*
Moderately/poorly	43	39.1	1.13 ± 2.27		
Disease Site					
Tongue	59	53.7	1.76 ± 2.45	*H = 1.820*	*0.769*
Gingival	10	9.1	1.35 ± 2.25		
Cheek	14	12.7	1.42 ± 2.05		
Floor of Mouth	15	13.6	1.17 ± 1.73		
Oropharynx	12	10.9	0.85 ± 2.11		
Recurrence					
Yes	19	17.3	1.98 ± 1.77	*Z = -1.372*	*0.170*
No	91	82.7	1.40 ± 2.33		

Abbreviations: OPN, osteopontin; SD, standard deviation; pN, pathological lymph node status; TNM stage, tumor-lymph node-metastasis stage.

[a]△Ct indicates the difference in the cycle number at which a sample's fluorescent signal passes a given threshold above baseline (Ct) derived from a specific gene compared with that of β-actin in tumor tissues.

Fibroblasts contribute to the up-regulation of OPN in HNC cells

The immunohistochemical staining of OPN in HNC tissues revealed that the OPN was primarily up-regulated in cancer cells and was slightly expressed in cancer stroma (Figure 2A). To further demonstrate the distribution of OPN in HNC tissues, we isolated NFs, CAFs and tumor cells from HNC tissues and adjacent normal tissues. The CAFs displayed an elongated, mesenchymal morphology and stained positive for the fibroblast markers Vimentin and α-SMA (Figure S3A, B). As previously reported [35], sequencing revealed no KRAS mutation in CAFs, indicating that these CAFs were truly of fibroblast origin (Figure S3C). The results of western blotting and real-time PCR indicated that OPN was highly expressed in tumor cells and increased OPN expression was also observed in CAFs compared to NFs (Figure 2B). Moreover, increased expression of OPN was detected in 8 HNC cell lines compared to normal oral epithelial cells at the protein and mRNA levels, as well as the secreted OPN level in cell culture supernatant (Figure 2C).

Table 2. Univariate and multivariate cox proportional hazards regression models for estimating overall survival

Characteristics	HR	95% CI	*P*
Univariate analysis			
Overall survival			
Age (< 60 y vs ≥ 60 y)	1.176	0.702 to 1.971	0.538
Gender (male vs female)	1.088	0.650 to 1.820	0.749
Smoking history (smoker vs nonsmoker)	1.546	0.921 to 2.596	0.100
Alcohol history (drinker vs nondrinker)	1.293	0.743 to 2.251	0.364
Tumor size (≤ 4 cm vs > 4 cm)	0.593	0.335 to 1.050	1.634
Lymph node metastasis (pN0 vs pN1 to pN2)	3.817	2.053 to 7.097	0.000
TNM stage	1.514	1.136 to 2.016	0.005
Pathological differentiation (Well vs Moderately to poorly)	1.427	0.816 to 2.496	0.012
Disease Site	1.125	0.938 to 1.350	0.203
Recurrence	1.784	0.929 to 3.423	0.082
OPN expression (high vs low)	3.958	2.097 to 7.471	0.000
Multivariate analysis			
Overall survival			
Lymph node metastasis (pN0 vs pN1 to pN2)	3.528	1.725 to 7.214	0.001
TNM stage	1.233	0.916 to 1.910	0.620
Pathological differentiation (Well vs Moderately to poorly)	1.177	0.676 to 2.047	0.476
OPN expression (high vs low)	3.629	1.790 to 7.357	0.000

Abbreviations: CI, confidence interval; HR, hazard ratio; pN, pathological lymph node status; TNM, tumor-lymph node-metastasis classification.

Interestingly, intense staining of OPN was observed in the peripheral cells of squamous cell carcinoma islands (Figure 2A), which suggested that the up-regulation of OPN in cancer cells might partly be due to the interactions between tumor cells and stromal cells. We have found that NFs could acquire the characteristics of CAFs to some extent after the interaction with tumor cells (Figure S4). In order to identify if CAFs promoted the expression of OPN in HNC cells, NFs were co-cultured with CAL-27 or SCC-25 cells (less OPN expression). Significant up-regulation of OPN was observed in CAL-27 or SCC-25 cells after co-culture with NFs (Figure 2D), while slightly increased OPN expression was detected in NFs co-cultured with cancer cells (Figure 2E). These data revealed that CAFs were sufficient to trigger the expression of OPN in cancer cells.

OPN accelerates the proliferation, migration and invasion of HNC cells

As a secreted protein, recombinant human OPN (rhOPN) was used to assess the effect of OPN on the proliferation and metastasis of HNC cells. The proliferation of CAL-27 and SCC-25 cells increased in a dose-dependent manner in response to rhOPN (Figure 3A, S5A), while the growth of HN4 and HN6 cells was inhibited following treatment with the OPN antibody (Figure 3B, S5B). Simultaneously, rhOPN drastically facilitated the migration and invasion of CAL-27 and SCC-25 cells (Figure 3C, S5C), while the OPN antibody partially decreased the migration and invasion of HN4 and HN6 cells (Figure 3D, S5D).

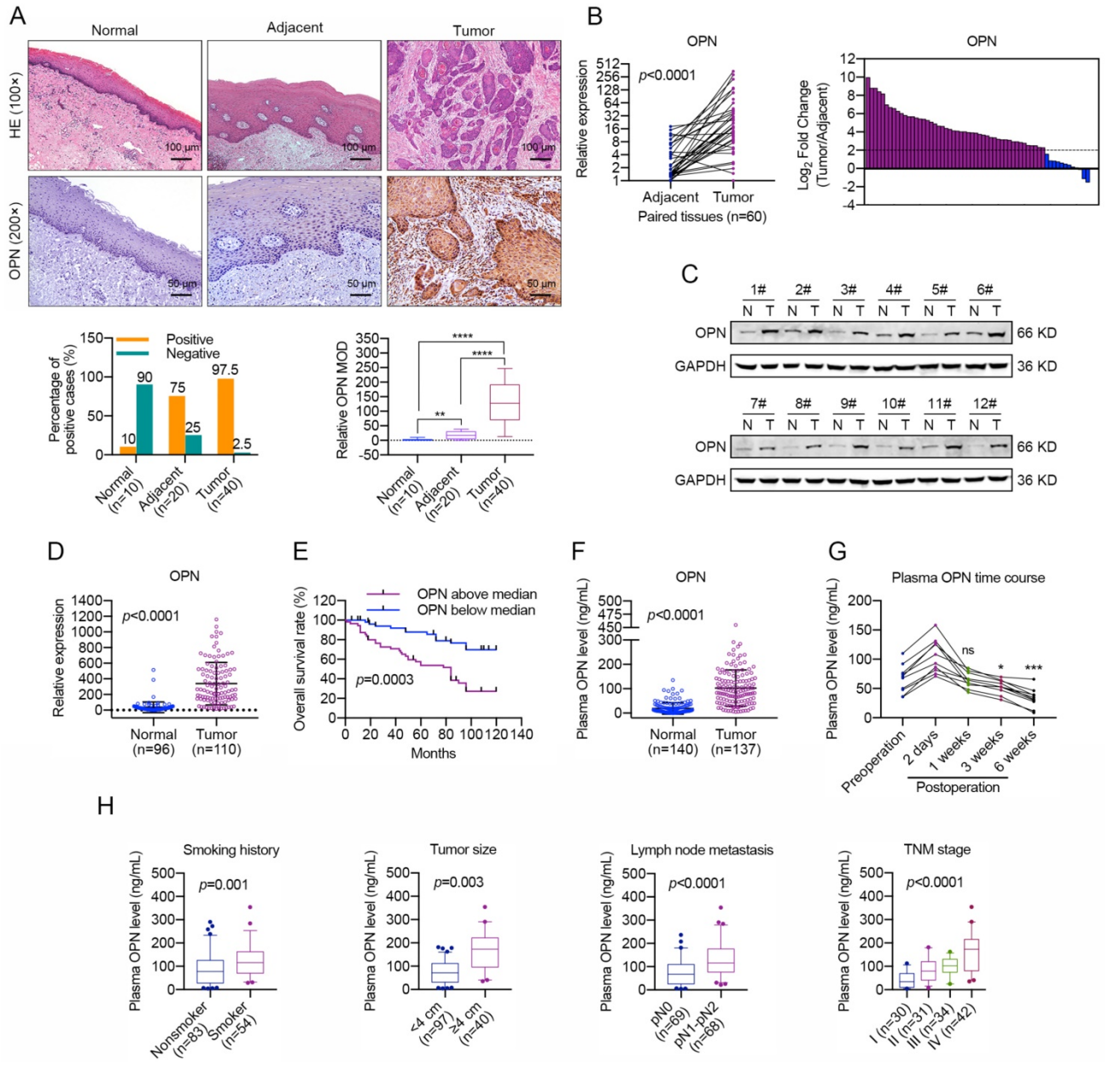

Figure 1. High OPN levels are associated with malignant transformation and lower overall survival in HNC. (A) Immunohistochemical analysis of OPN protein expression in normal oral epithelial tissues, HNC tissues and matched adjacent normal tissues. Homogenous brown cytoplasmic and membranous staining indicated positive expression, and significant OPN expression was observed in 97.5% (39/40) of tumor tissues, 75% (15/20) of adjacent normal tissues and 10% (1/10) of normal epithelial tissues (Scale bar, up: 100 μm; down: 50 μm). MOD, mean optical density. (B) The OPN expression and the comparison of OPN expression levels in 60 pairs of HNC samples and paired adjacent normal tissues. A log2-fold change more than 2 was regarded as significant up-regulation (dotted lines). (C) OPN protein levels were determined in 12 paired HNC samples using western blotting (N, adjacent normal tissue; T, tumor tissue). (D) OPN expression was determined using real-time PCR in 110 cases of HNC samples and in 96 cases of normal oral epithelial tissues. (E) Kaplan-Meier analyses of overall survival. Patients with high OPN expression had a significantly lower overall survival rate than patients with low OPN expression. (F) OPN plasma concentration (ng/mL) in HNC patients and healthy controls. (G) The plasma OPN concentration (ng/mL) of HNC patients before and after surgery (2 days, 1 week, 3 weeks and 6 weeks). (H) Higher plasma OPN levels were correlated with smoking, large tumor size, lymph node metastasis and advanced tumor stage in HNC. (ns, no significant difference; *p<0.05; **p<0.01; ***p<0.001; ****p<0.0001)

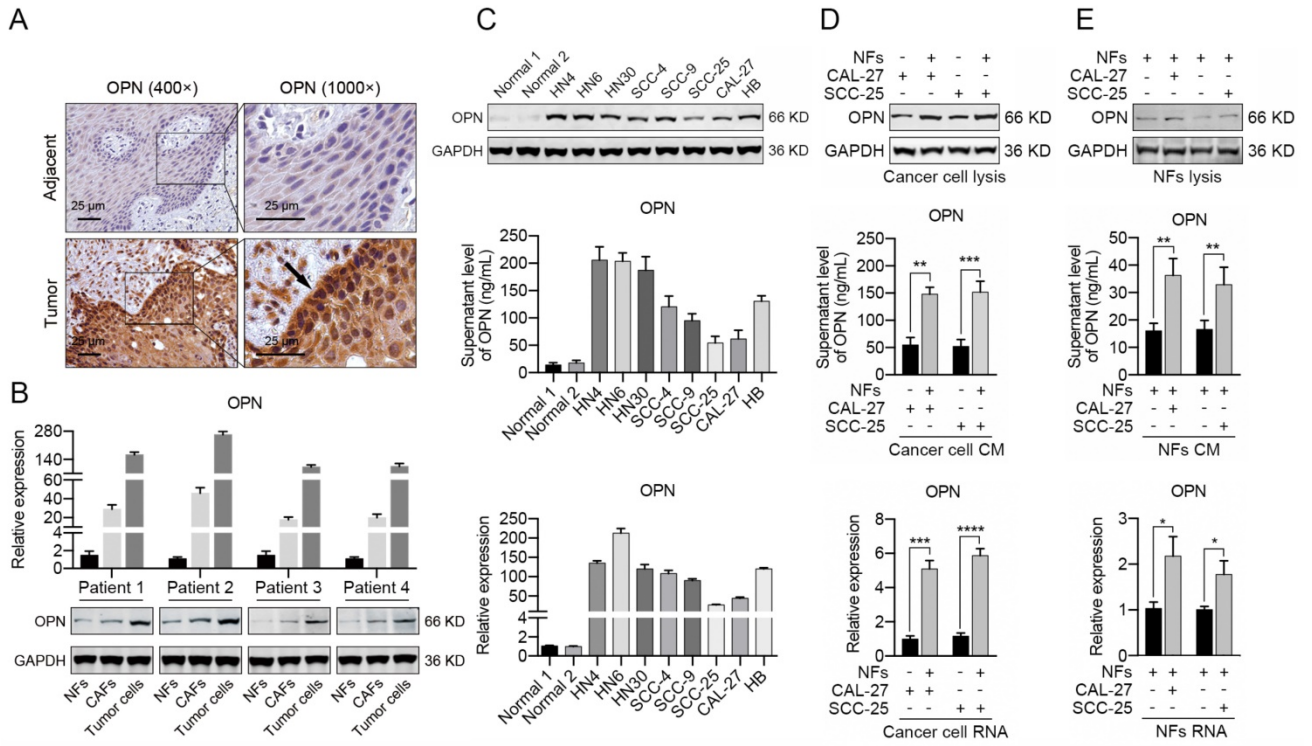

Figure 2. Fibroblasts contribute to the up-regulation of OPN in HNC cells. (A) Immunohistochemical analysis of OPN protein expression in HNC tissues and matched adjacent normal tissues (Scale bar: 25 μm). Higher staining of OPN was observed in tumor cells of the edge of bulk tumors. (B) The mRNA and protein levels of OPN were determined in NFs, CAFs and cancer cells (derived from 4 HNC patients) using real-time PCR and western blotting. (C) OPN at the protein and mRNA level and in the supernatant was detected in 8 representative HNC cell lines and normal oral epithelial cells (titled normal) using western blotting, real-time PCR and ELISA. (D) The protein level, supernatant concentration and mRNA level of OPN were determined in CAL-27 and SCC-25 cells after co-culture with NFs. (E) The protein level, supernatant concentration and mRNA level of OPN were determined in NFs after co-culture with CAL-27 and SCC-25 cells. (*p<0.05; **p<0.01; ***p<0.001; ****p<0.0001)

Furthermore, overexpression of OPN in CAL-27 and SCC-25 cells (Figure S6A, B) strongly promoted the proliferation (Figure 3E, S5E), migration, invasion and plate or soft agar colony-formation abilities of these cells (Figure 3G-I, S5G-I). Meanwhile, silencing of OPN by siRNA in HN4 and HN6 (Figure S6C, D) partially decreased the proliferation (Figure 3F, S5F), migration, invasion and colony-formation abilities of these cells (Figure 3J-L, S5J-L). Additionally, the wound healing assay also obtained the same conclusion (Figure S7). These results demonstrated that OPN promotes HNC progression.

CAF-derived IL-6 acts as a regulator of OPN expression

To further determine the mechanism of OPN expression in HNC cells, we detected the alterations in the expression levels of 10 genes (TGF-β1, TGF-β2, TGF-β3, IL-1A, IL-6, TNFα, PDGFA, PDGFB, FGF2 and EGF) that were reported to be soluble inducers of OPN [36-38] in NFs after the co-culture with HNC cells for 72 h. As a result, we found that TGF-β1, TGF-β2, TGF-β3 and IL-6 mRNAs were all substantially up-regulated in the co-cultured cancer cells and NFs (Figure 4A, B; S8A, B) using real-time PCR. Further investigations indicated that the mRNA levels of TGF-β1, TGF-β2, TGF-β3 and IL-6 were increased in HNC samples (Figure 4C, S9). Moreover, correlation analyses showed that there was a prominent positive correlation between OPN and IL-6 mRNA levels (Figure 4D, S9).

IL-6 was shown to be highly expressed by CAFs contacting different tumor types [15], indicating that CAFs might be the major source of IL-6 in tumor microenvironment. As shown in Figure S10A-C, IL-6 was significantly up-regulated in HNC tissues and higher IL-6 expression was observed in tumor stroma. In addition, HNC-derived CAFs expressed higher levels of IL-6 compared to NFs and cancer cells (Figure S10D, E), which revealed that IL-6 was primarily derived from CAFs in HNC.

To confirm that IL-6 was an upstream regulator of OPN, we used different concentration gradients of IL-6 to stimulate CAL-27 and SCC-25 cells and observed a dose-dependent increase of cellular OPN at both the mRNA and protein levels (Figure 4E, S8C). Furthermore, these effects were also detected in a time-dependent manner (Figure 4F, S8D). However, up- or down-regulation of OPN in HNC cell lines had no significant effect on IL-6 expression (Figure 4G, H; S8E, F). OPN expression is regulated by several

transcription factors, including NF-kappa B, c-Myc, OCT1, ETS1 and c-Jun [39-41]. Interestingly, chromatin immunoprecipitation analysis showed that part 1 (P1) of the OPN promoter exhibited a strong binding affinity with the STAT3 protein after IL-6 stimulation (Figure S11A, B). STAT3 inhibitor or STAT3-specific siRNAs partly inhibited the IL-6-induced OPN expression (Figure S11C, D). Moreover, the OPN up-regulation in HNC cells during co-culture with NFs was abrogated when IL-6 was blocked using an IL-6 antibody (Figure 4I, S8G), and the same results were obtained when NFs was transfected with specific IL-6 shRNA in advance (Figure 4J). Hence, these data confirmed that IL-6 was an upstream regulator of OPN.

As shown in Figure S12, IL-6 simulation was proved to notably facilitate the cell proliferation, migration and invasion of HNC cells *in vitro* and tumor metastasis *in vivo*. To further determine whether CAF-derived IL-6 could promote HNC progression via up-regulation of OPN in HNC cells, we mixed HNC cells stably expressing luciferase with NFs (tumor cells: NFs = 3:1), incubated the cells for 72 h and used them for various cellular analyses (Figure S8H). As shown in Figure 4K-M and S8I-K, both IL-6 antibody and OPN antibody antagonized the enhanced HNC cell growth, migration and invasion when co-cultured with NFs, and a combination of IL-6 and OPN antibody presented more significant results. Simultaneously, similar results were obtained when HNC cells were co-cultured with CAFs (Figure S13). In addition, both the promoting effects of NFs and CAFs on HNC cell growth, migration and invasion were remarkably reduced when the fibroblasts were transfected with shRNA targeting IL-6 in advance (Figure 4N, S14).

Collectively, these results indicated that IL-6 secreted by CAFs could promote HNC growth and metastasis via up-regulation of OPN in tumor cells.

Soluble OPN acts on HNC cells by binding the integrin receptor

OPN, a matricellular molecule, physiologically interacts with integrins (αvβ1, αvβ3, αvβ5) or CD44 to modulate the biological behaviors of cancers [42, 43]. In our present study, CAL-27 and SCC-25 cells were pre-treated with integrin antibodies for 1 h, and rhOPN (0.5 μM) was then added in the culture system. We found that the anti-αv or anti-β3 integrin antibodies partially decreased the effects of the rhOPN on HNC cell proliferation (Figure 5A). Moreover, the combination of anti-αv and anti-β3 integrin antibodies resulted in a more significant inhibition of HNC cell growth induced by rhOPN (Figure 5A). The endogenous interaction between OPN and integrin αvβ3 was further confirmed by co-IP (Figure 5B-D). Simultaneously, integrin αvβ3 antibody strongly antagonized the enhanced migration and invasion induced by rhOPN (Figure 5E, F). Hence, we confirmed that the tumor-promoting role of induced soluble OPN in HNC was primarily mediated by binding to integrin αvβ3.

The integrin αvβ3-NF-kappa B axis mediates OPN-induced HNC progression

We sought to determine the transcription factors involved in OPN-mediated HNC progression. Cumulative studies have reported that OPN enhances cell proliferation, cell motility and cancer stem cell-like phenotypes through activation of NF-kappa B in melanoma [25, 26], breast cancer [27, 44] and hepatocellular carcinoma [45]. Given that soluble OPN was involved in cell proliferation and motility in our present study, we investigated whether NF-kappa B also mediated OPN-induced HNC progression. To assess the effect of OPN on translocation of p65 into the nucleus, we treated CAL-27 and SCC-25 cells with 0.5 μM rhOPN in basal medium for 3 h at 37°C. Confocal microscopy analysis showed that complete nuclear accumulation of p65 was observed in CAL27 and SCC-25 cells after rhOPN treatment (Figure 6A, S15A). To determine whether the OPN-induced p65 translocation was inhibited by the selective NF-kappa B inhibitor pyrrolidine dithiocarbonate (PDTC), we pre-treated CAL27 and SCC-25 cells with 100 μM PDTC for 1 h and then treated them with 0.5 μM rhOPN for 3 h. The data indicated that PDTC inhibited OPN-induced nuclear translocation (Figure 6A, S15A), which further demonstrated that OPN could activate NF-kappa B signaling in HNC cells.

To further confirm that OPN induces p65 translocation, we prepared both the nuclear and cytoplasmic fractions from the indicated cancer cells. Western blot analyses revealed that p65 was localized mostly in the cytoplasm compared with the nucleus in control cells, while p65 was translocated from the cytoplasm to the nucleus after rhOPN treatment. Moreover, p65 was predominantly enriched in the cytoplasm when HNC cells were pre-treated with PDTC and then treated with rhOPN (Figure 6B, S15B). In addition, similar results were obtained when HNC cells were pre-treated with integrin αvβ3 antibody and then treated with rhOPN (Figure 6A, B; S15A, B). Moreover, rhOPN stimulated the phosphorylation and degradation of IκBα in HNC cells, which then promoted the phosphorylation of p65, and PDTC inhibited this process (Figure 6C, S15C). Meanwhile, overexpression of OPN in CAL-27 and SCC-25 cells also promoted the phosphorylation of IκBα and p65

(Figure 6D, S15D). These data demonstrated that OPN activated the NF-kappa B signaling pathway by binding with integrin αvβ3.

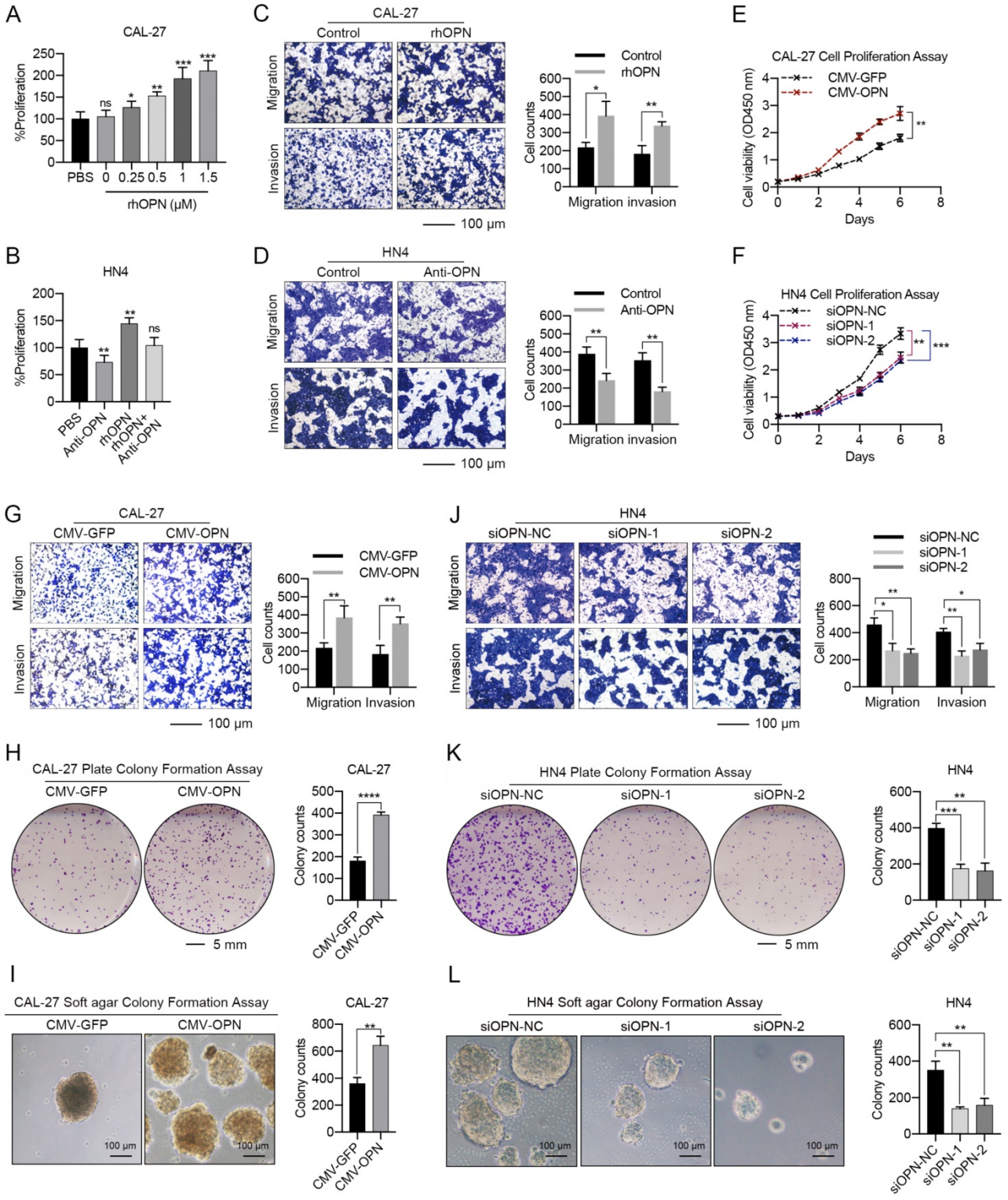

Figure 3. Functional analyses of the effects of OPN on HNC cell proliferation, migration and invasion. (A, B) Recombinant human OPN promoted the proliferation of CAL-27 cells in a dose-dependent manner, while neutralization of OPN with OPN antibody (5 μg/mL) inhibited the proliferation of HN4 cells. (C, D) Recombinant human OPN (0.5 μM) triggered the migration and invasion of CAL-27 cells, while OPN neutralizing antibody (5 μg/mL) inhibited the migration and invasion of HN4 cells. (E, F) Overexpression of OPN in CAL-27 cells facilitated the proliferation of tumor cells, while OPN knockdown in HN4 cells significantly inhibited the proliferative ability of tumor cells. (G-I) Overexpression of OPN in CAL-27 cells facilitated the migration, invasion, and plate and soft agar colony formation of tumor cells. (J-L) OPN knockdown with specific siRNA in HN4 cells significantly inhibited the migration, invasion and colony formation of tumor cells. (Scale bar, migration: 100 μm; invasion: 100 μm; plate colony formation: 5 mm; soft agar colony formation: 100 μm) (ns, no significant difference; *p<0.05; **p<0.01; ***p<0.001; ****p<0.0001)

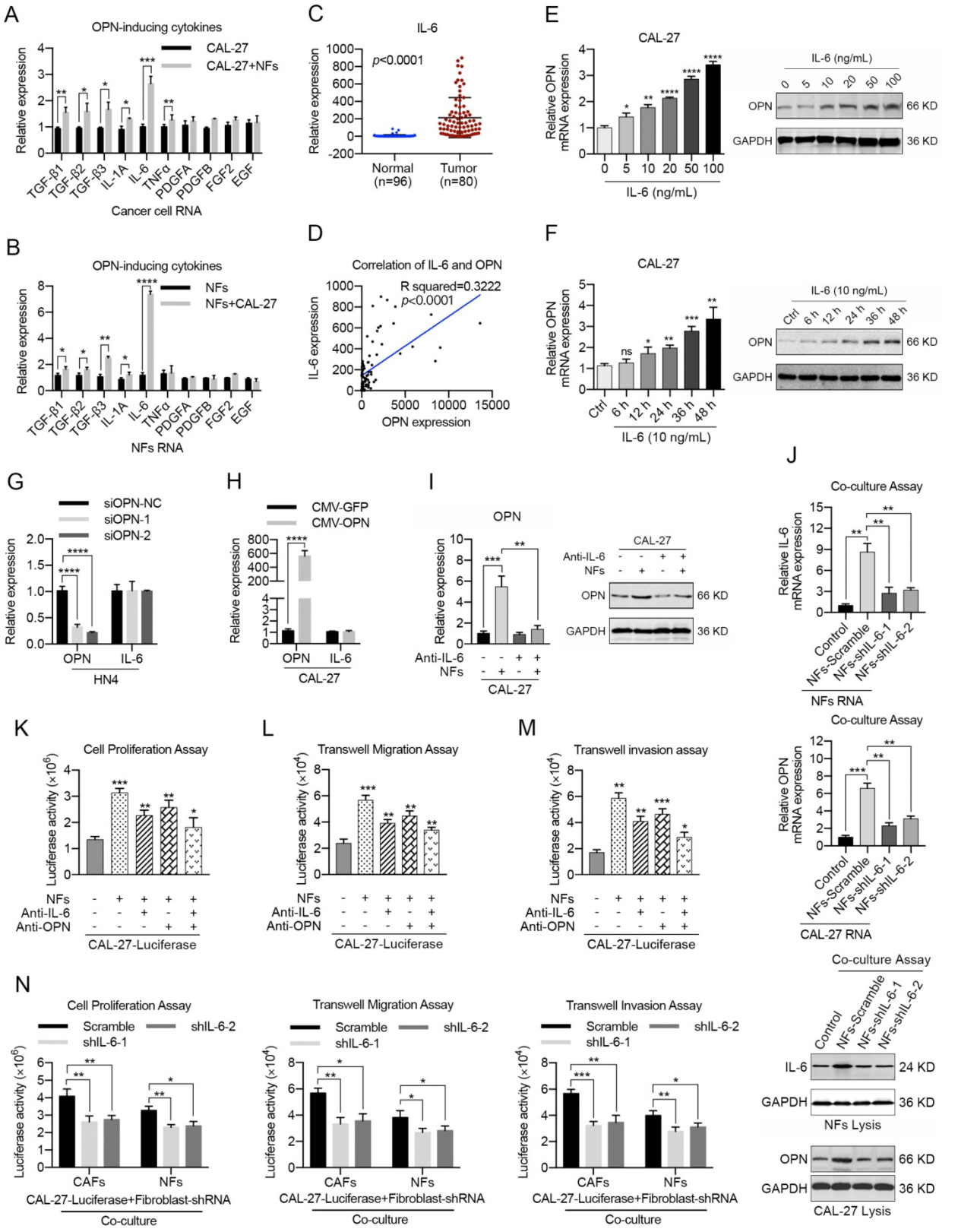

Figure 4. Stromal IL-6 induces the expression of neoplastic OPN during the interactions between HNC cells and fibroblasts. (A, B) The mRNA levels of TGF-β1, TGF-β2, TGF-β3, IL-1A, IL-6, TNFα, PDGFA, PDGFB, FGF2 and EGF in HNC cells (A) and NFs (B) were detected after the co-culture of NFs and CAL-27 cells by real-time PCR. (C, D) IL-6 mRNA levels were determined using real-time PCR in 80 HNC tissues and in 96 normal oral epithelial tissues. A significant positive correlation was observed between the IL-6 and OPN expression levels in the HNC tissues (n=80). (E, F) IL-6 induced OPN expression in CAL-27 cells in a dose-dependent and time-dependent manner. Protein expression by western blot analysis and mRNA expression by real-time PCR were measured at the indicated concentrations. (G, H) OPN overexpression in CAL-27 cells or OPN knockdown in HN4 cells showed little influence on IL-6 expression at the mRNA level. (I) The protein and mRNA levels of neoplastic OPN in CAL-27 cells were increased after co-culture with NFs and antagonized by IL-6-neutralizing antibody (5 μg/mL). (J) The protein and mRNA levels of IL-6 in NFs and OPN in CAL-27 cells were slightly increased after the co-culture of HNC cells and NFs transfected with shRNA targeting IL-6 in advance. (K-M) Both OPN (5 μg/mL) and IL-6 (5 μg/mL) neutralizing antibodies partially inhibited the NF-mediated proliferation, migration and invasion of CAL-27 cells, and the combination of OPN and IL-6 antibodies was superior to each of them alone. (N) The NF- or CAF-mediated proliferation, migration and invasion of CAL-27 cells were partly decreased when the fibroblasts were transfected with shRNA targeting IL-6 in advance. (*p<0.05; **p<0.01; ***p<0.001; ****p<0.0001)

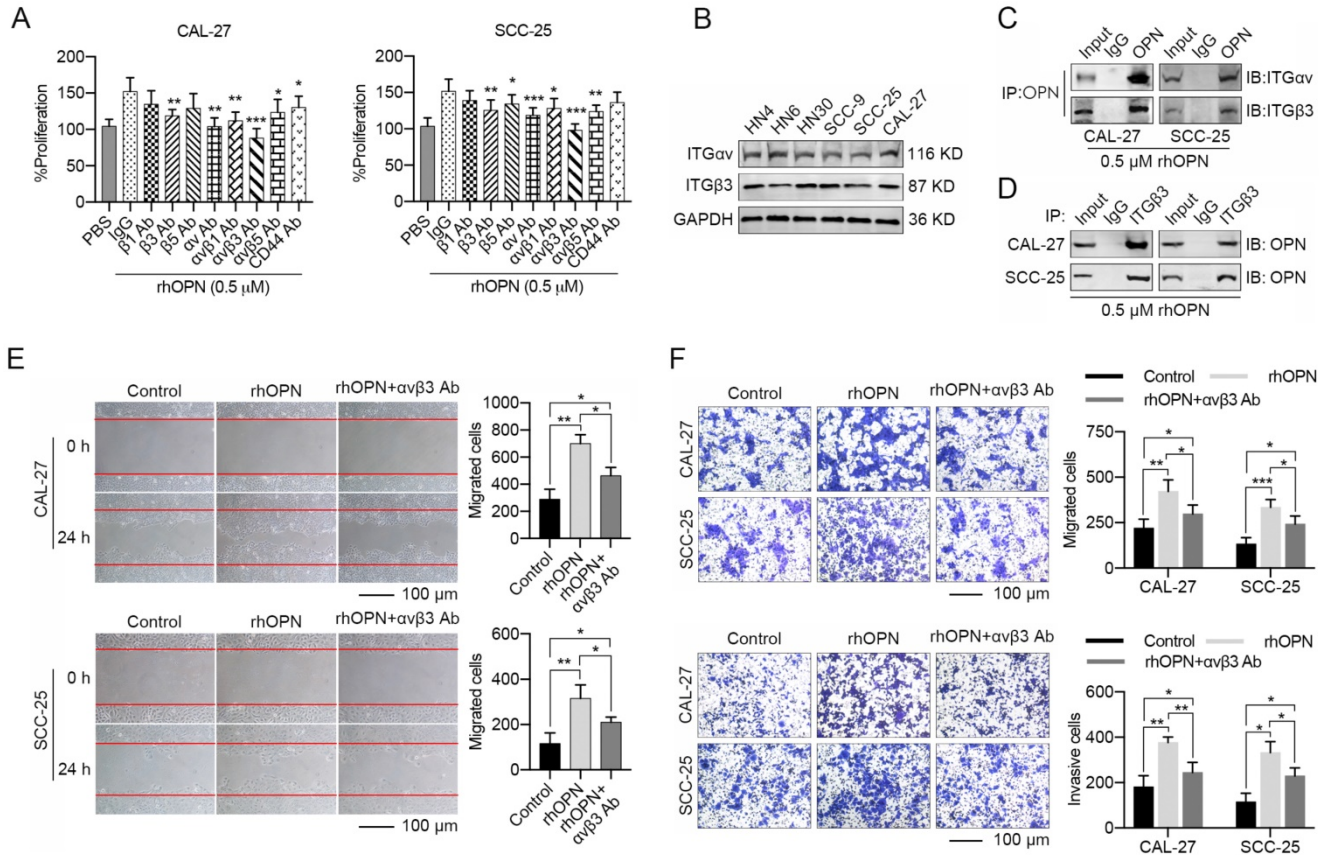

Figure 5. OPN exhibits its effects on HNC cells by binding an integrin receptor. (A) CAL-27 and SCC-25 cells were pre-treated with PBS, IgG (10 μg/mL), various integrin (integrin β1, β3, β5, αv, αvβ1, αvβ3 and αvβ5) antibodies (10 μg/mL) and CD44 antibody (10 μg/mL) for 1 h followed by treatment with 0.5 μM rhOPN for 48 h. The proliferative activities of these cells were measured using the CCK-8 method, and integrin αvβ3 antibody significantly inhibited the rhOPN-inducing tumor cell growth. (B) The protein levels of integrin αv and β3 in HN4, HN6, HN30, SCC-9, SCC-25 and CAL-27 cells. (C, D) CAL-27 and SCC-25 cells were pre-treated with 0.5 μM rhOPN for 3 h, and the interaction between OPN and integrin αvβ3 was confirmed via co-immunoprecipitation examination. (E, F) Recombinant human OPN (0.5 μM) promoted the migration and invasion of HNC cells, while blocking of integrin αv and β3 by integrin αvβ3 antibodies (10 μg/mL) inhibited the rhOPN-induced migration and invasion of HNC cells (Scale bar: 100 μm). (**p*<0.05; ***p*<0.01; ****p*<0.001)

The induction of NF-kappa B transcriptional activity by OPN was also monitored by luciferase reporter gene assays. As shown in Figure 6E and S15E, rhOPN stimulated the NF-kappa B transcriptional activity in HNC cells, and pretreatment with PDTC inhibited the OPN-induced NF-kappa B activity. Moreover, the conditioned medium (CM) from HNC cells with OPN overexpression dramatically increased the NF-kappa B transcriptional activity in 293T cells, and PTDC partly decreased the NF-kappa B activity (Figure 6E, S15E). Previous data have shown that OPN mediates increased expression of uPA, MMPs and ICAM-1, which are closely associated with cell growth and cell motility, via activation of NF-kappa B [25-27]. As a result, overexpression of OPN in HNC cells significantly stimulated the expression of MMP2, MMP9, uPA and ICAM-1 at the transcriptional level (Figure 6F, S15F). Similarly, the gene expression levels of MMP2, MMP9, uPA and ICAM-1 were up-regulated when stimulated by rhOPN, while PDTC inhibited the OPN-induced gene expression (Figure 6G, S15G). Functionally, the rhOPN-induced cell proliferation, cell migration and invasion were suppressed by PDTC (Figure 6H, S15H).

These data indicated that OPN could promote HNC cell proliferation, migration and invasion through the integrin αvβ3-NF-kappa B axis. More importantly, the malignant phenotypes of HNC cells induced by IL-6 could be partially blocked by inhibition of OPN function by siRNA, antibody against OPN or αvβ3 integrin, or PDTC (Figure 7). In summary, we carefully concluded that IL-6 could facilitate HNC cell progression via the OPN-αvβ3-NF-kappa B pathway *in vitro*.

IL-6 mediated induction of OPN promotes the proliferation and metastasis of HNC cells *in vivo*

To determine whether the induced OPN affected tumorigenicity and metastasis *in vivo*, we overexpressed OPN in CAL-27 cells and found that it promoted xenograft tumor growth and higher plasma OPN level (Figure 8A, B). To further illustrate the

effects of OPN on IL-6-induced tumor growth, we mixed NFs and CAL-27 cells and subcutaneously injected the cells to establish a xenograft model. We found that treatment with an OPN neutralizing antibody blocked the stimulatory effects of IL-6 on tumor growth *in vivo*, and the OPN antibody combined with IL-6 antibody showed more significant inhibition of the xenograft tumor growth than the single antibody groups (Figure 8C). Interestingly, a similar trend in plasma OPN level was observed in these nude mice (Figure 8D). Immunohistochemical staining revealed that the expression levels of nuclear p65, Ki-67, MMP2, MMP9, uPA and ICAM-1 were higher in the CAL-27-OPN group and CAL-27+NFs group than the control group or OPN antibody treatment group (Figure S16). Moreover, exogenous OPN expression in Rca-T cells accelerated the formation and growth of the metastatic nodules, and increased OPN was observed in the plasma (Figure 8E, F). These *in vivo* experiments further demonstrated that the IL-6-induced OPN could promote the growth and metastasis of HNC via the NF-kappa B signaling pathway.

A combination of OPN and IL-6 serves as a powerful prognostic and diagnostic factor for HNC patients

Considering the effects of IL-6 on OPN expression, we established a predictive mRNA panel of OPN and IL-6 by using logistic regression. The predicted probability of HNC diagnosis from the logit model based on the OPN and IL-6 mRNA panel, logit (p=HNC) = -5.667+0.623×OPN+0.609×IL-6, was used for survival analysis and the construction of a receiver operating characteristic (ROC) curve. The 5-year overall survival rates of HNC patients in the low OPN group, low IL-6 group and low combination group were 87.8%, 84.3% and 88.3%, respectively. The survival rates in high OPN group, high IL-6 group and high combination group were 53.5%, 55.6% and 46.8%, respectively (Figure 1E, 8G and S17A). The above data revealed that the OPN and IL-6 mRNA panel showed improved prediction of overall survival in HNC compared to either parameter alone.

Given the increased plasma IL-6 level and the correlation between plasma IL-6 level and OPN level (Figure S17B, C), we also constructed a predictive panel of plasma OPN and IL-6 in patients diagnosed with HNC [logit (p=HNC) = -3.171+0.04×OPN+0.13× IL-6]. Thereafter, ROC curves were constructed to evaluate the OPN performance as a marker for discriminating the 5-year survival group from the death group, the TNM stage I group from the healthy controls and the metastasis group from the non-metastasis group in HNC patients. ROC curves were also used to assess whether addition of IL-6 improved the model. The analysis demonstrated that the OPN and IL-6 mRNA panel had high accuracy in discriminating the 5-year survival group from the death group [panel: AUC=0.849 (95% CI, 0.775-0.923); OPN: AUC=0.764 (95% CI, 0.666-0.863); IL-6: AUC=0.736 (95% CI, 0.642-0.830)], the TNM stage I group from the health controls [panel: AUC=0.887 (95% CI, 0.813-0.961); OPN: AUC=0.846 (95% CI, 0.756-0.936); IL-6: AUC=0.871 (95% CI, 0.789-0.953)] and the metastasis group from the non-metastasis group [panel: AUC=0.884 (95% CI, 0.820-0.948); OPN: AUC=0.784 (95% CI, 0.700-0.868); IL-6: AUC=0.862 (95% CI, 0.792-0.932)] compared with OPN or IL-6 alone (Figure 8H-J, S17D-F). In addition, similar results were obtained when assessing the plasma OPN and IL-6 panel (Figure S17G, H). Overall, these data indicate that the combination of OPN and IL-6 could serve as a more accurate prognostic and diagnostic factor for HNC patients.

Discussion

Cancer, with its multifactorial nature and complex heterogeneity, is responsible for high mortality rates worldwide [1]. OPN, a secreted and matrix-specific molecule, was reported to be up-regulated in numerous cancers and plays an important role in tumor progression by modulating the cancer signaling pathways and the tumor microenvironment [8, 9, 11]. Although the tumor-promoting role of OPN has been widely accepted, several studies have reported an anti-tumorigenic function of OPN in tumor progression [46, 47]. However, there is still a lack of evidence systematically demonstrating the tumor-supporting role of OPN in HNC. In the present study, we confirmed that OPN was up-regulated in HNC specimens (including tumor tissues and plasma obtained from HNC patients) and cancer cell lines. Thereafter, overexpression of OPN in HNC tissues or increased plasma OPN level was shown to be correlated with high-grade malignancies and associated with poor prognosis, respectively. Moreover, the elevated OPN promoted the proliferation, colony formation, migration and invasion of HNC cells *in vitro* and *in vivo*. We confirmed that overexpression of OPN contributed to tumor malignancy and poor outcomes in HNC, which indicated that OPN might be a promising prognostic biomarker and therapeutic target for HNC. Small-molecule inhibitors or aptamers specifically targeting OPN or OPN-related genes have recently been described, although further studies are required to establish them as potentially useful cancer treatments.

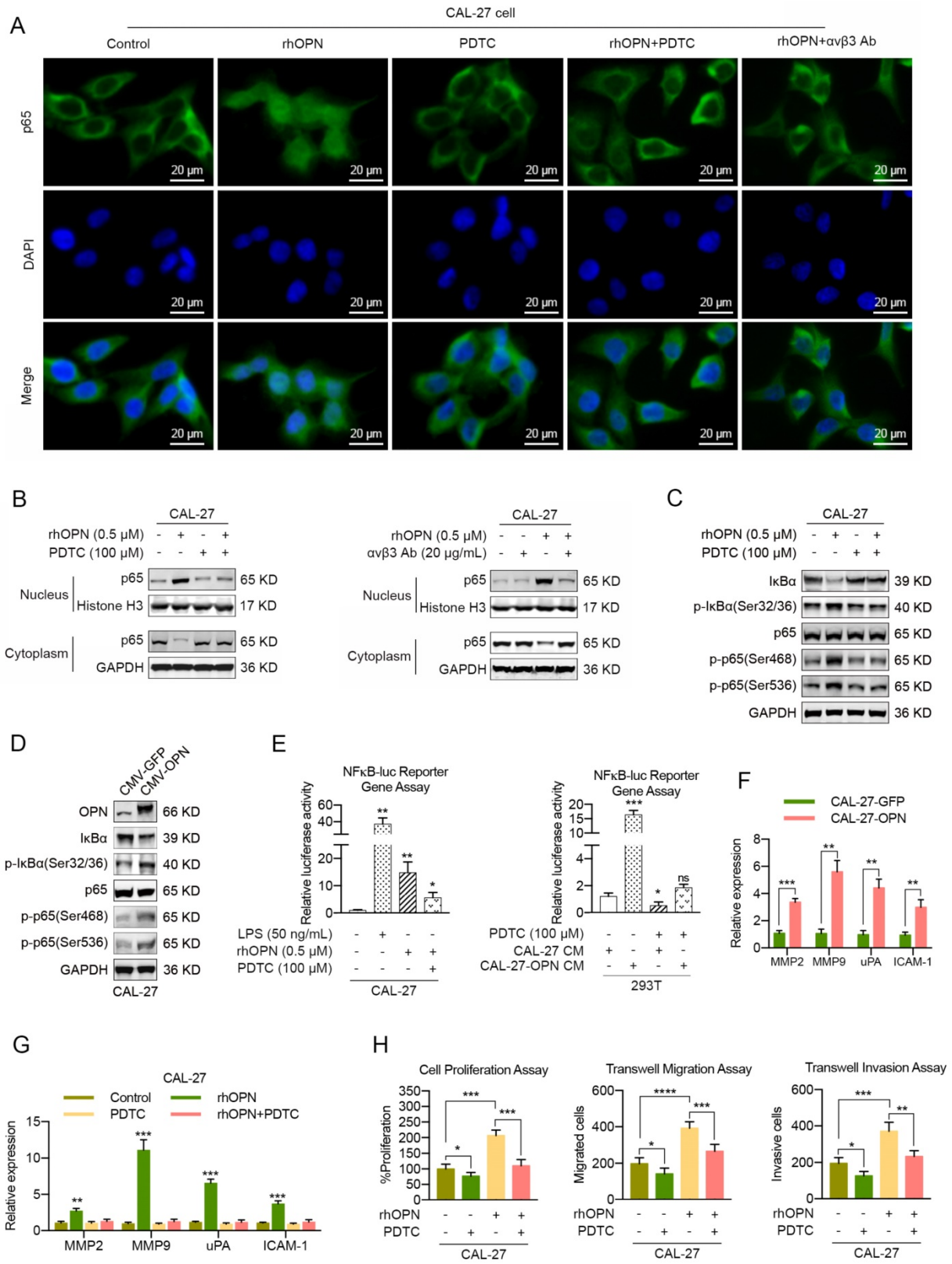

Figure 6. OPN promotes the proliferation, migration and invasion of HNC cells through the integrin αvβ3-NF-kappa B axis. (A, B) CAL-27 cells were treated with 0.5 μM rhOPN for 3 h or pre-treated with 100 μM PDTC or 20 μg/mL integrin αvβ3 antibody for 1 h followed by treatment with 0.5 μM rhOPN for 3 h. Immunofluorescence assays and western blot analysis were used to assess the location of p65 in CAL-27 cells (Scale bar: 20 μm). (C, D) Western blot analysis of IκBα degradation, phosphorylated IκBα (Ser 32/36), p65 and phosphorylated p65 (Ser 468 and Ser 536) in CAL-27 cells following treatment with rhOPN or OPN overexpression. (E) Constitutive NF-kappa B-response promoter activity. Recombinant human OPN, as well as OPN-enriched CM stimulated the NF-kappa B transcriptional activity, and pretreatment with PDTC partly inhibited this effect. LPS (50 ng/mL) was used as a positive control. (F) OPN overexpression in CAL-27 cells stimulated the mRNA expression of MMP2, MMP9, uPA and ICAM-1. (G) Recombinant human OPN directly induced the expressions of MMP2, MMP9, uPA and ICAM-1 in CAL-27 cells, and the expressions were partially suppressed when pre-treated with PDTC. (H) The OPN-induced CAL-27 cell growth, migration and invasion were partially neutralized by pretreatment with PDTC. (ns, no significant difference; *p<0.05; **p<0.01; ***p<0.001; ****p<0.0001)

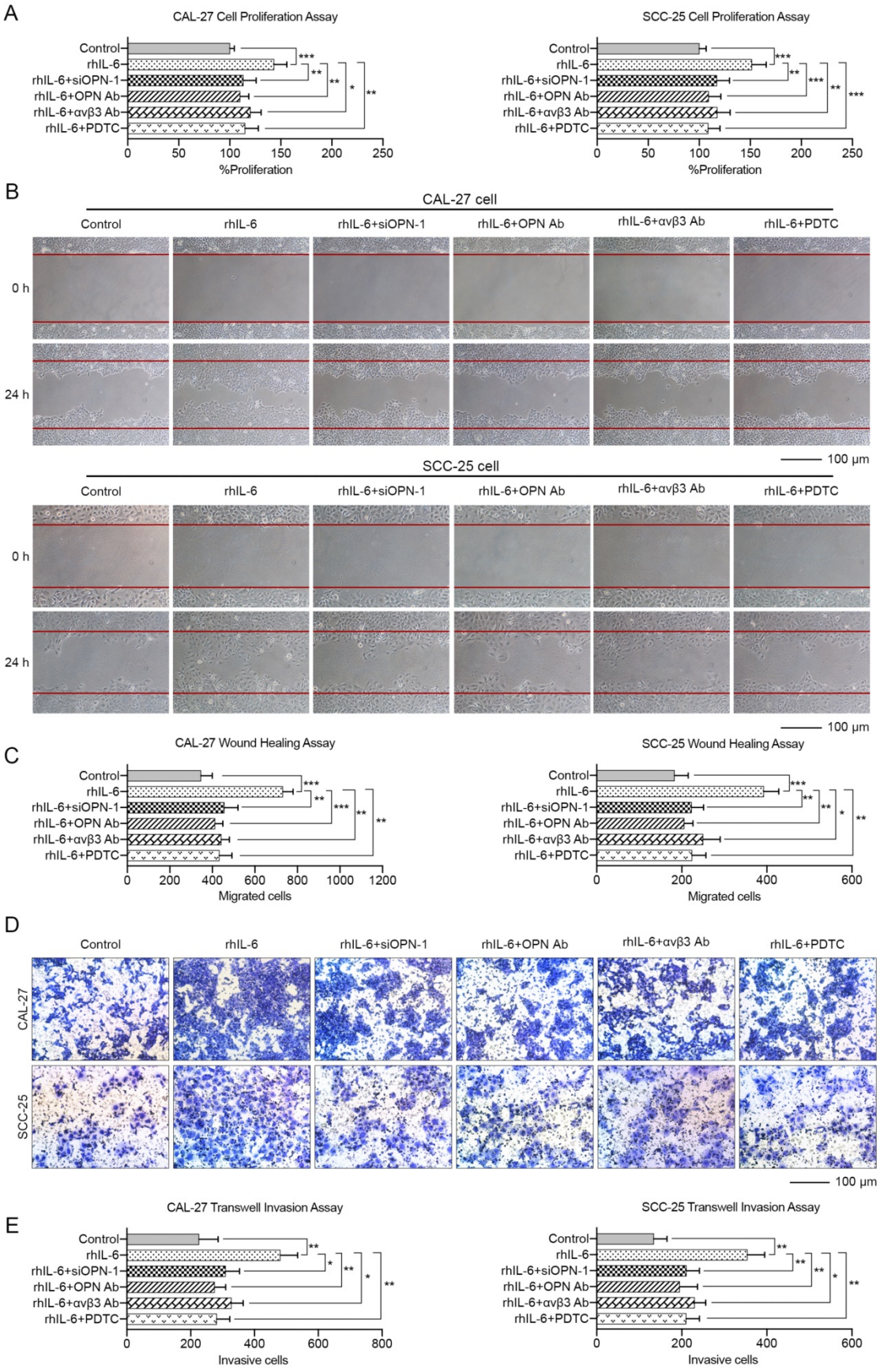

Figure 7. OPN contributes to IL-6 mediated proliferation, migration and invasion of HNC. CAL-27 and SCC-25 cells were treated with 10 ng/mL rhIL-6 for 72 h or pre-treated with 50 nM siOPN-1, 5 μg/mL OPN antibody, 20 μg/mL integrin αvβ3 antibody or 100 μM PDTC for 6 h followed by addition of 10 ng/mL rhIL-6 and incubation for 72 h. Cell proliferation assay (A), wound healing assay (B, C) and transwell invasion assay (D, E) were implemented to analyze the alterations in tumor cell growth, migration and invasion among different groups (Scale bar: 100 μm). (*p<0.05; **p<0.01; ***p<0.001)

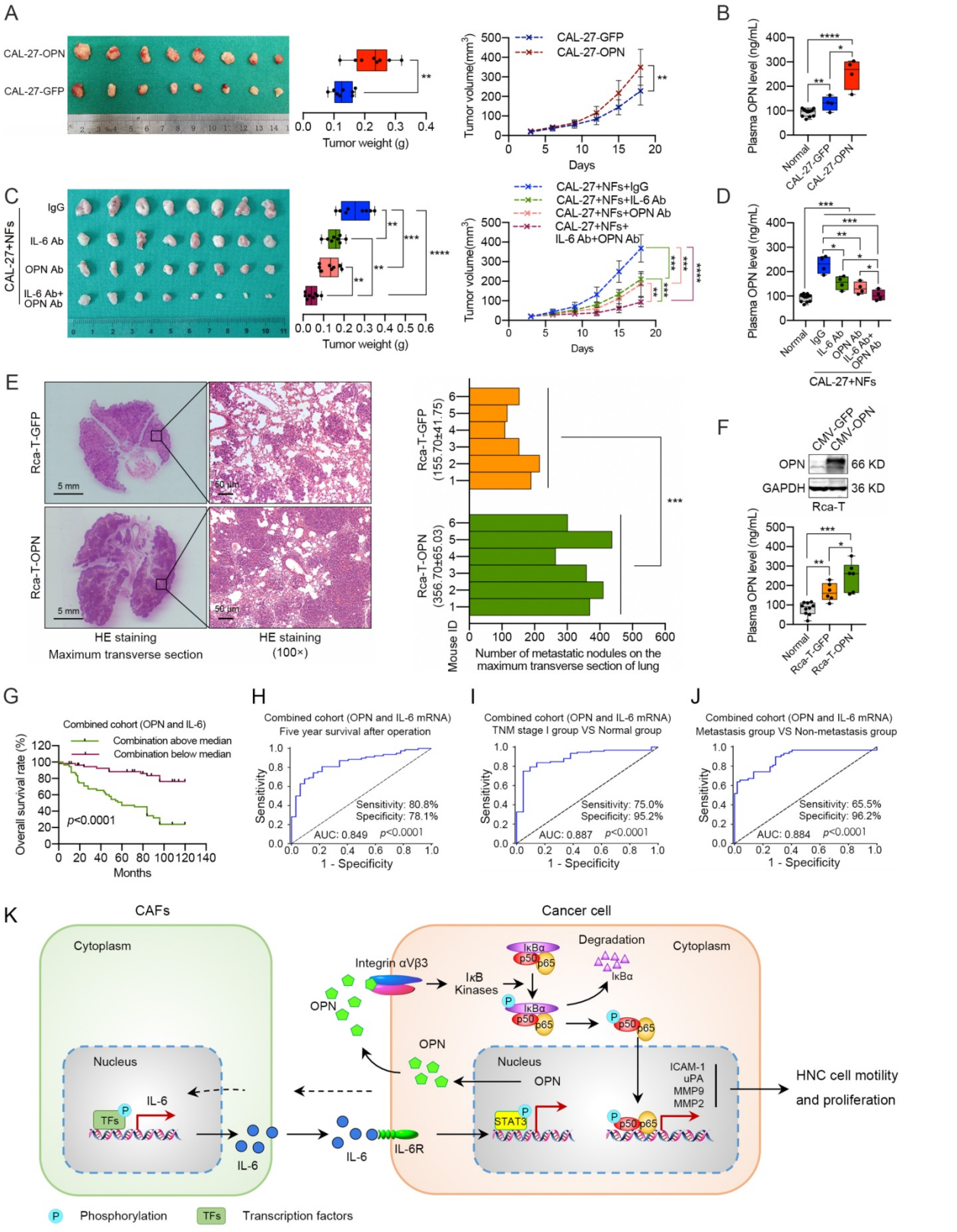

Figure 8. Effects of stromal IL-6-induced OPN on promoting tumor growth and metastasis *in vivo*. (A) OPN overexpression in CAL-27 cells facilitated the xenograft tumor growth in nude mice. (B) Plasma OPN levels of the tumor-bearing mice from the normal group, CAL-27 group and CAL-27-OPN group. (C) Subcutaneous injection of OPN antibody (10 μg per tumor nodule) or IL-6 antibody (10 μg per tumor nodule) around the tumor partly inhibited NF-mediated tumor growth, and the combination of OPN antibody (5 μg per tumor nodule) and IL-6 antibody (5 μg per tumor nodule) exhibited a more powerful antitumor activity. (D) Plasma OPN levels of the tumor-bearing mice from the normal group, IgG treatment group, OPN antibody treatment group, IL-6 antibody treatment group and the combination group. (E) Overexpression of OPN in Rca-T cells promoted the formation and growth of metastatic nodules in nude mice (Scale bar, left: 5 mm; right: 100 μm). (F) Western blot analysis confirmed the exogenous expression of OPN in Rca-T cells, and plasma OPN levels of the mice involved in experimental metastasis were measured using ELISA. (G) Kaplan-Meier analyses of overall survival. (H, I and J) ROC curve analysis of the mRNA panel of OPN and IL-6 stratified by different groups in the validation set. ROC plots for the mRNA panel of OPN and IL-6 discriminated the five-year survival group from the death group (H), the TNM stage I group from the healthy controls (I), and the metastasis group from the non-metastasis group (J). AUC, area under the curve. (K) A proposed model illustrating the modulatory role of stromal IL-6-induced neoplastic OPN in controlling tumor growth and metastasis. (*p<0.05; **p<0.01; ***p<0.001; ****p<0.0001)

OPN plays an important role in the pathogenesis of various inflammatory diseases and has been classified as a cytokine based on its proinflammatory properties [48]. OPN expression is always up-regulated during inflammation, immune response and various other conditions [9, 25, 49]. During this study, we found that both OPN expression in HNC tissues and plasma OPN levels were higher in smokers than non-smokers. Smoking was reported to promote oxidative stress and local or systemic chronic inflammation, and OPN is a well-documented inflammatory marker [50]. Furthermore, the plasma OPN levels decreased after smoking cessation [50]. In addition, our results suggest that both tumor size and the postsurgical condition can result in significantly increased plasma OPN levels. Instead of the anticipated immediate postoperative decrease, we observed a prominent elevation of plasma OPN within 2 days and a return to preoperative values approximately 3 weeks thereafter. The difference in plasma OPN based on time from resection is likely due to the important role of OPN in wound healing, local inflammation and the systemic stress response after surgery [51, 52]. Moreover, the decreased plasma OPN level of HNC patients 6 weeks after surgery further revealed that tumor cells and interactions within the tumor microenvironment contributed to the increased plasma OPN levels in HNC patients. Hence, plasma OPN could serve as a powerful prognostic and diagnostic biomarker for HNC. However, more studies should be carried out to eliminate the interference from other factors during the studies on plasma OPN given the complicated role of OPN in pathophysiology.

CAFs, the activated fibroblasts in tumor stroma, are the most abundant cells in the tumor microenvironment, play a prominent role in tumor progression and are regarded as a promising tool in cancer therapeutics [14, 53]. Compared with NFs, CAFs significantly facilitate the growth, migration, invasion, angiogenesis and chemoresistance of many cancer types [54]. Previous studies have shown that CAFs secrete a plethora of factors that promote the growth and invasion of the underlying tumor [14]. IL-6, a multifunctional cytokine produced predominantly by CAFs in the tumor microenvironment, was reported as a direct critical driver of tumor growth and metastasis [55]. In this study, we revealed that IL-6 was increased in both plasma and cancer tissue of HNC patients, and significantly higher expression was found in CAFs. The CAF-derived IL-6 induced the expression of OPN in tumor cells, and the elevated OPN then promoted the growth and metastasis of HNC cells. However, many questions remain as to whether the increased OPN is induced by activation of the IL-6 signaling pathway rather than being a concomitant phenomenon, as IL-6 promotes epithelial-mesenchymal transition in cancer cells directly to facilitate tumor metastasis [56]. Thus, we further analyzed our data to answer this question. First, depletion of soluble OPN proteins dramatically attenuated the effect of IL-6 in HNC cells. Second, the currently available data indicate that IL-6 triggers IL-6 trans-signaling to up-regulate the expression of OPN in macrophages and tumor cells [38, 57], and we demonstrated that STAT3 bound to the OPN promoter after IL-6 stimulation. Third, the IL-6 expression in clinical samples exhibited a positive correlation with OPN expression. Finally, we identified IL-6 as the key regulator of OPN expression in the HNC microenvironment by screening a panel of cytokines. Hence, we concluded that IL-6 could accelerate the proliferation, migration and invasion of HNC by regulating the OPN expression. Simultaneously, our present data would be a supplement to the mechanisms of IL-6-related tumor progression.

IL-6 was reported to promote the growth of tumor cells in many types of human cancer [58]. Interestingly, it was also revealed that IL-6 has an inhibitory effect on some tumor cells [58]. There are two viewpoints about the effect of IL-6 on the HNC cell proliferation *in vitro*. It was reported that neither tocilizumab (IL-6R antibody) nor exogenous IL-6 influenced the proliferation rate of HNC cells independently of treatment time [59]. Meanwhile, some studies revealed that IL-6 could promote the proliferation of HNC cells *in vitro* and blocking IL-6 signaling significantly decreased the proliferative rates of these cells [60-62]. In this study, we found that rhIL-6 promoted HNC cells growth *in vitro* and IL-6 antibody inhibited the proliferation of HNC cells. We think that this conflicting impact of IL-6 on HNC cell proliferation *in vitro* might be due to the different genetic background and origins of these cell types and whether IL-6 induces proliferation of HNC cells also may depend on the specific cellular context.

Tumor progression is driven not only by aberrant mutations or dysregulation of genes in tumor cells but also by the different types of stromal cells [63]. OPN is highly increased in stromal cells present within the tumor microenvironment. Stroma-derived OPN was reported to play a crucial role in tumorigenicity, metastasis and angiogenesis [22, 64, 65]. Previous studies have revealed that fibroblasts were induced to produce OPN either by direct interaction with tumor cells or by soluble factors derived from the tumor cells [66]. In this study, we demonstrated that OPN was primarily located in

tumor cells, and CAFs expressed higher OPN levels than NFs. Moreover, increased OPN expression was observed in NFs after co-culture with HNC cells. With regard to the mechanisms of augmented OPN production, our data suggested that OPN production in fibroblasts was induced by direct interaction with HNC cells or with soluble factors derived from HNC cells. We identified IL-6 as a key regulator of tumor-derived OPN in HNC. However, we failed to detect significant up-regulation of OPN in fibroblasts when treated with rhIL-6, suggesting that other molecule(s) might be involved in OPN production of fibroblasts. Hence, a series of experiments should be performed to determine the key regulatory factors of fibroblast-derived OPN in future studies.

Here, our data showed that OPN contributes to HNC growth and metastasis via the integrin αvβ3-NF-kappa B axis. OPN promotes tumor malignant transformation primarily by binding integrin or CD44 receptors, which activate multiple signaling pathways that regulate the expression of various oncogenic molecules [8, 10]. Among these receptors, we found that the integrin αvβ3 antibody strongly inhibited the OPN-mediated growth, migration and invasion of HNC cells. A large body of evidence has suggested that the NF-kappa B pathway contributes to the development of several types of human cancer, including HNC. Moreover, our previous study demonstrated that increased NF-kappa B activity was associated with HNC metastasis, and OPN depletion resulted in suppression of NF-kappa B activity [67]. Therefore, we hypothesized that the proinflammatory factor OPN could activate NF-kappa B signaling via interaction with integrin αvβ3, and our results confirmed this hypothesis. However, this mechanism only partly illustrates the regulatory role of OPN in HNC progression, and more efforts are needed to further elucidate the roles of OPN.

OPN, especially plasma OPN, has been reported to be a promising prognostic factor in many cancers, including HNC [9, 52]. In this study, we showed that OPN and IL-6 were both powerful prognostic and diagnostic factors for HNC patients. Moreover, the combination of plasma IL-6 and OPN had a better prognostic and diagnostic performance than IL-6 or OPN alone. However, we found that the diagnostic efficiency of the plasma OPN and IL-6 was not as good as that of their mRNA levels in tumor tissue. OPN and IL-6 are both inflammatory factors that are secreted by immune cells, stromal cells and other cell types, and the plasma levels of OPN and IL-6 can be affected by local and systemic factors of the human body [56, 68]. These factors may affect the prognostic and diagnostic efficiency of plasma OPN and IL-6. Hence, stricter inclusion criteria should be established to determine the true prognostic and diagnostic efficiency of OPN and IL-6 in future studies.

Taken together, the results showed that OPN was up-regulated in HNC and associated with poor clinical outcomes. Moreover, our study highlights the role of OPN in promoting HNC cell growth, migration and invasion and has identified CAF-derived IL-6 by screening a panel of cytokines as a key regulator of neoplastic OPN expression in the tumor microenvironment. In HNCs, the neoplastic OPN directly accelerated NF-kappa B activity by binding to integrin αvβ3 and indirectly modulating the tumor-promoting microenvironment for HNC progression by up-regulating the expression of MMPs, uPA and ICAM-1 in tumor cells (Figure 8K). As a result, the combination of IL-6 and OPN may be a promising prognostic and diagnostic indicator and a potential therapeutic target for HNC patients.

Abbreviations

HNC: Head and neck cancer; OPN: Osteopontin; ECM: extracellular matrix; TGF-β: transforming growth factor-β; IL-1α: interleukin-1α; IL-6: interleukin-6; TNF-α: tumor necrosis factor-α; PDGF: platelet derived growth factor; FGF2: fibroblast growth factor 2; EGF: epidermal growth factor; CAFs: cancer-associated fibroblasts; NFs: normal fibroblasts; CM: conditioned medium; EMT: epithelial-mesenchymal transition.

Supplementary Material

Supplementary methods, figures and tables. These materials show the detailed experimental procedures, the identification of CAFs, the functional roles of CAFs and IL-6 in HNC progression, the diagnostic values of OPN and IL-6 in HNC, and the primers used for real-time PCR.
http://www.thno.org/v08p0921s1.pdf

Acknowledgements

This work was supported by the National Program on Key Research Project of China (2016YFC0902700), the National Natural Science Foundation of China (81772933, 81472572 and 91229103), Shanghai Municipal Science and Technology Commission Funded Project (15DZ2292300 and 15QA1402800), the Fundamental Research Funds for the Central Universities (Ninth People's Hospital, Shanghai Jiao Tong University School of Medicine, Jianjun Zhang) and the Innovation Fund for Doctoral Program of Shanghai Jiao Tong University, School of Medicine (BXJ201727).

Competing Interests

The authors have declared that no competing interest exists.

References

1. Siegel RL, Miller KD, Jemal A. Cancer statistics, 2016. CA Cancer J Clin. 2016; 66: 7-30.
2. Kao SY, Mao L, Jian XC, Rajan G, Yu GY. Expert Consensus on the Detection and Screening of Oral Cancer and Precancer. Chin J Dent Res. 2015; 18: 79-83.
3. Sacco AG, Cohen EE. Current Treatment Options for Recurrent or Metastatic Head and Neck Squamous Cell Carcinoma. J Clin Oncol. 2015; 33: 3305-13.
4. Senger DR, Wirth DF, Hynes RO. Transformed mammalian cells secrete specific proteins and phosphoproteins. Cell. 1979; 16: 885-93.
5. Franzen A, Heinegard D. Isolation and characterization of two sialoproteins present only in bone calcified matrix. Biochem J. 1985; 232: 715-24.
6. Ishijima M, Rittling SR, Yamashita T, Tsuji K, Kurosawa H, Nifuji A, et al. Enhancement of osteoclastic bone resorption and suppression of osteoblastic bone formation in response to reduced mechanical stress do not occur in the absence of osteopontin. J Exp Med. 2001; 193: 399-404.
7. Diao H, Kon S, Iwabuchi K, Kimura C, Morimoto J, Ito D, et al. Osteopontin as a mediator of NKT cell function in T cell-mediated liver diseases. Immunity. 2004; 21: 539-50.
8. El-Tanani MK. Role of osteopontin in cellular signaling and metastatic phenotype. Front Biosci. 2008; 13: 4276-84.
9. Rangaswami H, Bulbule A, Kundu GC. Osteopontin: role in cell signaling and cancer progression. Trends Cell Biol. 2006; 16: 79-87.
10. Ahmed M, Sottnik JL, Dancik GM, Sahu D, Hansel DE, Theodorescu D, et al. An Osteopontin/CD44 Axis in RhoGDI2-Mediated Metastasis Suppression. Cancer Cell. 2016; 30: 432-43.
11. Bandopadhyay M, Bulbule A, Butti R, Chakraborty G, Ghorpade P, Ghosh P, et al. Osteopontin as a therapeutic target for cancer. Expert Opin Ther Targets. 2014; 18: 883-95.
12. Weber GF, Lett GS, Haubein NC. Osteopontin is a marker for cancer aggressiveness and patient survival. Br J Cancer. 2010; 103: 861-9.
13. Petrik D, Lavori PW, Cao H, Zhu Y, Wong P, Christofferson E, et al. Plasma osteopontin is an independent prognostic marker for head and neck cancers. J Clin Oncol. 2006; 24: 5291-7.
14. Kalluri R, Zeisberg M. Fibroblasts in cancer. Nat Rev Cancer. 2006; 6: 392-401.
15. Cirri P, Chiarugi P. Cancer associated fibroblasts: the dark side of the coin. Am J Cancer Res. 2011; 1: 482-97.
16. McAllister SS, Gifford AM, Greiner AL, Kelleher SP, Saelzler MP, Ince TA, et al. Systemic endocrine instigation of indolent tumor growth requires osteopontin. Cell. 2008; 133: 994-1005.
17. Anderberg C, Li H, Fredriksson L, Andrae J, Betsholtz C, Li X, et al. Paracrine signaling by platelet-derived growth factor-CC promotes tumor growth by recruitment of cancer-associated fibroblasts. Cancer Res. 2009; 69: 369-78.
18. Weber CE, Kothari AN, Wai PY, Li NY, Driver J, Zapf MA, et al. Osteopontin mediates an MZF1-TGF-beta1-dependent transformation of mesenchymal stem cells into cancer-associated fibroblasts in breast cancer. Oncogene. 2015; 34: 4821-33.
19. Kale S, Raja R, Thorat D, Soundararajan G, Patil TV, Kundu GC. Osteopontin signaling upregulates cyclooxygenase-2 expression in tumor-associated macrophages leading to enhanced angiogenesis and melanoma growth via alpha9beta1 integrin. Oncogene. 2015; 34: 5408-10.
20. Pazolli E, Luo X, Brehm S, Carbery K, Chung JJ, Prior JL, et al. Senescent stromal-derived osteopontin promotes preneoplastic cell growth. Cancer Res. 2009; 69: 1230-9.
21. Zhou Y, Dai DL, Martinka M, Su M, Zhang Y, Campos EI, et al. Osteopontin expression correlates with melanoma invasion. J Invest Dermatol. 2005; 124: 1044-52.
22. Song J, Ge Z, Yang X, Luo Q, Wang C, You H, et al. Hepatic stellate cells activated by acidic tumor microenvironment promote the metastasis of hepatocellular carcinoma via osteopontin. Cancer Lett. 2015; 356: 713-20.
23. Pikarsky E, Porat RM, Stein I, Abramovitch R, Amit S, Kasem S, et al. NF-kappaB functions as a tumour promoter in inflammation-associated cancer. Nature. 2004; 431: 461-6.
24. Zandi E, Rothwarf DM, Delhase M, Hayakawa M, Karin M. The IkappaB kinase complex (IKK) contains two kinase subunits, IKKalpha and IKKbeta, necessary for IkappaB phosphorylation and NF-kappaB activation. Cell. 1997; 91: 243-52.
25. Rangaswami H, Bulbule A, Kundu GC. Nuclear factor-inducing kinase plays a crucial role in osteopontin-induced MAPK/IkappaBalpha kinase-dependent nuclear factor kappaB-mediated promatrix metalloproteinase-9 activation. J Biol Chem. 2004; 279: 38921-35.
26. Philip S, Kundu GC. Osteopontin induces nuclear factor kappa B-mediated promatrix metalloproteinase-2 activation through I kappa B alpha /IKK signaling pathways, and curcumin (diferulolylmethane) down-regulates these pathways. J Biol Chem. 2003; 278: 14487-97.
27. Ahmed M, Kundu GC. Osteopontin selectively regulates p70S6K/mTOR phosphorylation leading to NF-kappaB dependent AP-1-mediated ICAM-1 expression in breast cancer cells. Mol Cancer. 2010; 9: 101.
28. Sun SJ, Wu CC, Sheu GT, Chang HY, Chen MY, Lin YY, et al. Integrin beta3 and CD44 levels determine the effects of the OPN-a splicing variant on lung cancer cell growth. Oncotarget. 2016; 7: 55572-84.
29. Wu X, Cao W, Wang X, Zhang J, Lv Z, Qin X, et al. TGM3, a candidate tumor suppressor gene, contributes to human head and neck cancer. Mol Cancer. 2013; 12: 151.
30. Zhong LP, Pan HY, Zhou XJ, Ye DX, Zhang L, Yang X, et al. Characteristics of a cancerous cell line, HIOEC-B(a)P-96, induced by benzo(a)pyrene from human immortalized oral epithelial cell line. Arch Oral Biol. 2008; 53: 443-52.
31. Jiang C, Ye D, Qiu W, Zhang X, Zhang Z, He D, et al. Response of lymphocyte subsets and cytokines to Shenyang prescription in Sprague-Dawley rats with tongue squamous cell carcinomas induced by 4NQO. BMC Cancer. 2007; 7: 40.
32. Lv Z, Wu X, Cao W, Shen Z, Wang L, Xie F, et al. Parathyroid hormone-related protein serves as a prognostic indicator in oral squamous cell carcinoma. J Exp Clin Cancer Res. 2014; 33: 100.
33. Naito S, von Eschenbach AC, Giavazzi R, Fidler IJ. Growth and metastasis of tumor cells isolated from a human renal cell carcinoma implanted into different organs of nude mice. Cancer Res. 1986; 46: 4109-15.
34. Qin X, Yan M, Zhang J, Wang X, Shen Z, Lv Z, et al. TGFbeta3-mediated induction of Periostin facilitates head and neck cancer growth and is associated with metastasis. Sci Rep. 2016; 6: 20587.
35. Richards KE, Zeleniak AE, Fishel ML, Wu J, Littlepage LE, Hill R. Cancer-associated fibroblast exosomes regulate survival and proliferation of pancreatic cancer cells. Oncogene. 2017; 36: 1770-8.
36. Wang X, Louden C, Ohlstein EH, Stadel JM, Gu JL, Yue TL. Osteopontin expression in platelet-derived growth factor-stimulated vascular smooth muscle cells and carotid artery after balloon angioplasty. Arterioscler Thromb Vasc Biol. 1996; 16: 1365-72.
37. Noda M, Vogel RL, Craig AM, Prahl J, DeLuca HF, Denhardt DT. Identification of a DNA sequence responsible for binding of the 1,25-dihydroxyvitamin D3 receptor and 1,25-dihydroxyvitamin D3 enhancement of mouse secreted phosphoprotein 1 (SPP-1 or osteopontin) gene expression. Proc Natl Acad Sci U S A. 1990; 87: 9995-9.
38. Wang CQ, Sun HT, Gao XM, Ren N, Sheng YY, Wang Z, et al. Interleukin-6 enhances cancer stemness and promotes metastasis of hepatocellular carcinoma via up-regulating osteopontin expression. Am J Cancer Res. 2016; 6: 1873-89.
39. Zhao W, Wang L, Zhang M, Wang P, Zhang L, Yuan C, et al. NF-kappaB- and AP-1-mediated DNA looping regulates osteopontin transcription in endotoxin-stimulated murine macrophages. J Immunol. 2011; 186: 3173-9.
40. Sato M, Morii E, Komori T, Kawahata H, Sugimoto M, Terai K, et al. Transcriptional regulation of osteopontin gene in vivo by PEBP2alphaA/CBFA1 and ETS1 in the skeletal tissues. Oncogene. 1998; 17: 1517-25.
41. Wang D, Yamamoto S, Hijiya N, Benveniste EN, Gladson CL. Transcriptional regulation of the human osteopontin promoter: functional analysis and DNA-protein interactions. Oncogene. 2000; 19: 5801-9.
42. Uede T. Osteopontin, intrinsic tissue regulator of intractable inflammatory diseases. Pathol Int. 2011; 61: 265-80.
43. Weber GF, Ashkar S, Glimcher MJ, Cantor H. Receptor-ligand interaction between CD44 and osteopontin (Eta-1). Science. 1996; 271: 509-12.
44. Das R, Mahabeleshwar GH, Kundu GC. Osteopontin stimulates cell motility and nuclear factor kappaB-mediated secretion of urokinase type plasminogen activator through phosphatidylinositol 3-kinase/Akt signaling pathways in breast cancer cells. J Biol Chem. 2003; 278: 28593-606.
45. Cao L, Fan X, Jing W, Liang Y, Chen R, Liu Y, et al. Osteopontin promotes a cancer stem cell-like phenotype in hepatocellular carcinoma cells via an integrin-NF-kappaB-HIF-1alpha pathway. Oncotarget. 2015; 6: 6627-40.
46. Crawford HC, Matrisian LM, Liaw L. Distinct roles of osteopontin in host defense activity and tumor survival during squamous cell carcinoma progression in vivo. Cancer Res. 1998; 58: 5206-15.
47. Bourassa B, Monaghan S, Rittling SR. Impaired anti-tumor cytotoxicity of macrophages from osteopontin-deficient mice. Cell Immunol. 2004; 227: 1-11.
48. Uede T, Katagiri Y, Iizuka J, Murakami M. Osteopontin, a coordinator of host defense system: a cytokine or an extracellular adhesive protein? Microbiol Immunol. 1997; 41: 641-8.
49. Rangaswami H, Bulbule A, Kundu GC. JNK1 differentially regulates osteopontin-induced nuclear factor-inducing kinase/MEKK1-dependent activating protein-1-mediated promatrix metalloproteinase-9 activation. J Biol Chem. 2005; 280: 19381-92.
50. Bishop E, Theophilus EH, Fearon IM. In vitro and clinical studies examining the expression of osteopontin in cigarette smoke-exposed endothelial cells and cigarette smokers. BMC Cardiovasc Disord. 2012; 12: 75.
51. Park JE, Barbul A. Understanding the role of immune regulation in wound healing. Am J Surg. 2004; 187: 11S-6S.
52. Blasberg JD, Pass HI, Goparaju CM, Flores RM, Lee S, Donington JS. Reduction of elevated plasma osteopontin levels with resection of non-small-cell lung cancer. J Clin Oncol. 2010; 28: 936-41.
53. De Vlieghere E, Verset L, Demetter P, Bracke M, De Wever O. Cancer-associated fibroblasts as target and tool in cancer therapeutics and diagnostics. Virchows Arch. 2015; 467: 367-82.
54. Shiga K, Hara M, Nagasaki T, Sato T, Takahashi H, Takeyama H. Cancer-Associated Fibroblasts: Their Characteristics and Their Roles in Tumor Growth. Cancers (Basel). 2015; 7: 2443-58.

55. Grivennikov SI, Greten FR, Karin M. Immunity, inflammation, and cancer. Cell. 2010; 140: 883-99.
56. Yadav A, Kumar B, Datta J, Teknos TN, Kumar P. IL-6 promotes head and neck tumor metastasis by inducing epithelial-mesenchymal transition via the JAK-STAT3-SNAIL signaling pathway. Mol Cancer Res. 2011; 9: 1658-67.
57. Uchibori T, Matsuda K, Shimodaira T, Sugano M, Uehara T, Honda T. IL-6 trans-signaling is another pathway to upregulate Osteopontin. Cytokine. 2017; 90: 88-95.
58. Hong DS, Angelo LS, Kurzrock R. Interleukin-6 and its receptor in cancer: implications for translational therapeutics. Cancer. 2007; 110: 1911-28.
59. Shinriki S, Jono H, Ota K, Ueda M, Kudo M, Ota T, et al. Humanized anti-interleukin-6 receptor antibody suppresses tumor angiogenesis and in vivo growth of human oral squamous cell carcinoma. Clin Cancer Res. 2009; 15: 5426-34.
60. Hong SH, Ondrey FG, Avis IM, Chen Z, Loukinova E, Cavanaugh PF, Jr., et al. Cyclooxygenase regulates human oropharyngeal carcinomas via the proinflammatory cytokine IL-6: a general role for inflammation? FASEB J. 2000; 14: 1499-507.
61. Bran G, Gotte K, Riedel K, Hormann K, Riedel F. IL-6 antisense-mediated growth inhibition in a head and neck squamous cell carcinoma cell line. In Vivo. 2011; 25: 579-84.
62. Chen MF, Wang WH, Lin PY, Lee KD, Chen WC. Significance of the TGF-beta1/IL-6 axis in oral cancer. Clin Sci (Lond). 2012; 122: 459-72.
63. Quail DF, Joyce JA. Microenvironmental regulation of tumor progression and metastasis. Nat Med. 2013; 19: 1423-37.
64. Kale S, Raja R, Thorat D, Soundararajan G, Patil TV, Kundu GC. Osteopontin signaling upregulates cyclooxygenase-2 expression in tumor-associated macrophages leading to enhanced angiogenesis and melanoma growth via alpha9beta1 integrin. Oncogene. 2014; 33: 2295-306.
65. Kumar S, Sharma P, Kumar D, Chakraborty G, Gorain M, Kundu GC. Functional characterization of stromal osteopontin in melanoma progression and metastasis. PloS one. 2013; 8: e69116.
66. Ota D, Kanayama M, Matsui Y, Ito K, Maeda N, Kutomi G, et al. Tumor-alpha9beta1 integrin-mediated signaling induces breast cancer growth and lymphatic metastasis via the recruitment of cancer-associated fibroblasts. J Mol Med (Berl). 2014; 92: 1271-81.
67. Yan M, Xu Q, Zhang P, Zhou XJ, Zhang ZY, Chen WT. Correlation of NF-kappaB signal pathway with tumor metastasis of human head and neck squamous cell carcinoma. BMC Cancer. 2010; 10: 437.
68. Sodek J, Ganss B, McKee MD. Osteopontin. Crit Rev Oral Biol Med. 2000; 11: 279-303.